

Quark Mass Hierarchy, FCNC and CP violation in a Seesaw model

Y. Kiyo¹, T. Morozumi¹, P.Parada^{2,3}, M.N.Rebelo^{3,4} and M.Tanimoto^{4,5}

1. Dept. of Physics, Hiroshima University, 739-8526 Higashi-Hiroshima, Japan.
2. Dep. de Física, Universidade da Beira Interior, Rua Marquês d'Ávila e Bolama, 6200 Covilhã, Portugal.
3. CFIF/IST, Av. Rovisco Pais, P-1096 Lisboa Codex, Portugal.
4. Dep. de Física, Instituto Superior Técnico, Av. Rovisco Pais, P-1096 Lisboa Codex, Portugal.
5. Science Education Laboratory, Ehime University, Bunkyo-cho, 790-8577 Matsuyama, Japan.

Abstract

The seesaw model of quark masses is studied systematically, focusing on its developments. A framework allowing the top quark mass to be of the order of the electroweak symmetry breaking scale, while the remaining light quarks have much smaller masses, due to the seesaw mechanism, is presented. The violation of the GIM mechanism is shown to be small and the tree level FCNC are suppressed naturally. In this model, there are many particles which could contribute to the FCNC in the one-loop level. Parameters of the model are constrained by using the experimental data on $K^0 - \bar{K}^0$ mixing and ϵ_K . The rare K meson decays $K_{L,S} \rightarrow \pi^0 \nu \bar{\nu}$ and $K^+ \rightarrow \pi^+ \nu \bar{\nu}$ are also investigated in the model. In these processes the scalar operators $(\bar{s}d)(\bar{\nu}_\tau \nu_\tau)$, which are derived from box diagrams in the model, play an important role due to an enhancement factor M_K/m_s in the matrix element $\langle \pi | \bar{s}d | K \rangle$. It is emphasized that the K_L decay process through the scalar operator is not the CP violating mode, so $B(K_L \rightarrow \pi^0 \nu \bar{\nu})$ remains non-zero even in the CP conserved limit. The pion energy spectra for these processes are predicted.

1 Introduction

The idea of the seesaw mechanism for the neutrino mass [1] [2] was extended to quark masses sometime ago [3]-[7]. At that time, the top quark mass was not known and it was not expected to be as heavy as the electroweak symmetry breaking scale. Therefore all charged fermions were assumed to be lighter than 10^2 GeV. The motivation for the construction of the model was to give an explanation for the smallness of the masses of the charged fermions (quarks and charged leptons) as compared to the electroweak breaking scale. However, now we know that

the top quark is as heavy as $O(10^2 \text{ GeV})$ and that has to be taken into account. Koide and Fusaoka (KF) [8] and T. Morozumi, T. Satou, M. N. Rebelo and M. Tanimoto [9] studied the top quark mass problem in a seesaw model. Based on this successful approach, we can discuss implications of the seesaw model focusing on the experimental data such as flavor changing neutral currents (FCNC) and CP violation. In this paper, we present in detail the formalism and make a systematic phenomenological analysis of the implications of the model. A brief introduction to the Dirac seesaw scheme is given in section 2, in which the incorporation of the top quark is outlined. In section 3 we show how the mass hierarchy and the flavor mixing are introduced. Section 4 is devoted to estimating tree level FCNC. In section 5, the flavor mixing in the charged currents is studied and the parameterization of the generalized Cabibbo Kobayashi Maskawa (CKM) matrix is specified. [16] [17] In section 6, the $K^0 - \bar{K}^0$ mixing and the CP violating parameter ϵ_K are studied and the constraint on the parameters of the present model is obtained. In section 7, the rare K meson decays $K \rightarrow \pi \nu \bar{\nu}$ are studied in the present model. The effect of the scalar interaction on the resulting pion energy spectrum is given. Our conclusions are presented in section 8.

2 Seesaw Model and Top Quark Mass

Let us first summarize the ideas of the seesaw model for quark masses. The gauge group of the standard model (SM) is extended to $SU(2)_L \times SU(2)_R \times U(1)$, so that the usual Yukawa mass terms for the charged fermions are not allowed, since now the right handed charged fermions belong to an $SU(2)_R$ doublet. That is:

$$\delta_{SU(2)_R} (\bar{\psi}_L \phi d_R) \neq 0. \quad (1)$$

The $SU(2)_R$ gauge boson must be much heavier than the $SU(2)_L$ gauge boson because we do not see any deviation from the V-A structure of the charged currents, thus the symmetry has to be broken at a sufficiently high energy scale. The representation of the Higgs breaking $SU(2)_R$ is chosen in such a way that no renormalizable mass term for the standard-like fermions is allowed. Therefore, for example, the Higgs bi-doublet $M(2, 2)$ under $SU(2)_L \times SU(2)_R$ is excluded. A single Higgs doublet, $\phi_R(1, 2)$, is used for breaking $SU(2)_R$. With this Higgs field, the possible mass term for the standard-like quarks is the dimension 5 operator,

$$\frac{1}{\Lambda_{NEW}} \bar{\psi}_L \phi_L \phi_R^\dagger \psi_R, \quad (2)$$

where Λ_{NEW} is some new physics scale. The scale must be larger than η_R (VEV of ϕ_R). Quarks and charged leptons acquire their masses, which are much smaller than the electroweak breaking scale, η_L (i.e., VEV of ϕ_L), through the dimension 5 operator:

$$m_f = \frac{\eta_L \eta_R}{\Lambda_{NEW}}, \quad (3)$$

where $\frac{\eta_R}{\Lambda_{NEW}} \ll 1$. Now we can think of what is the fundamental theory behind this dimension 5 operator. The interaction can be reproduced if we introduce new heavy isosinglet quarks (and

charged leptons) and integrate them out. These isosinglet quarks can have bare mass terms, and the new physics scale, Λ_{NEW} , is identified with that mass. Such a renormalizable theory is given, in the quark sector, by the following Lagrangian terms:

$$\mathcal{L} = -y_L \bar{\psi}_L \phi_L U_R - y_R \bar{\psi}_R \phi_R U_L + (h.c.) - M_U \bar{U} U. \quad (4)$$

Using this Lagrangian, we may compute the Feynman diagram in which the heavy singlet quark is exchanged, obtaining for the dimension 5 operator:

$$\frac{1}{\Lambda_{NEW}} = \frac{y_L y_R^*}{M_U}. \quad (5)$$

However this formula leads to the suppression of the quark masses by a factor of $SU(2)_R$ breaking scale divided by Singlet quark mass compared to the electroweak breaking scale, hence it cannot be applied to the top quark. In order to prevent the seesaw mechanism to act for the top quark we assume that the corresponding singlet quark has a bare mass much smaller than the $SU(2)_R$ breaking scale. In this case, ignoring flavor mixing for the moment, the top quark only acquires mass through a dimension 4 Yukawa coupling, instead of the mechanism of exchange of a heavy singlet quark. To illustrate, let us consider the extreme limit in which the bare mass is set to zero in Eq.(4), so that we have

$$\mathcal{L} = -y_L \eta_L \bar{t}_L T_R - y_R^* \eta_R \bar{T}_L t_R + (h.c.). \quad (6)$$

These are dimension 4 operators and the singlet quark cannot be integrated out because the bare mass term is absent. The diagonalization is performed through maximal mixing for the right-handed sector, as follows:

$$\begin{aligned} \begin{pmatrix} t^m \\ T^m \end{pmatrix}_L &= \begin{pmatrix} t \\ T \end{pmatrix}_L, \\ \begin{pmatrix} t^m \\ T^m \end{pmatrix}_R &= \begin{pmatrix} T \\ t \end{pmatrix}_R, \end{aligned} \quad (7)$$

(the superscript m denoting the mass states), leading to:

$$m_t = |y_L| \eta_L, \quad m_T = |y_R| \eta_R, \quad (8)$$

and m_t is of the order of the experimental value. If we retain the bare mass term, i.e., $-M_T \bar{T} T$, the mass formulae are given by

$$\begin{aligned} m_t &= |y_L| |y_R| \frac{\eta_L \eta_R}{\sqrt{|y_R|^2 \eta_R^2 + M_T^2}}, \\ m_T &= \sqrt{|y_R|^2 \eta_R^2 + M_T^2}. \end{aligned} \quad (9)$$

3 Quark Mass Hierarchy and Flavor Mixing

We will now extend our analysis to the case where flavor mixing is present and the number of generations is three, based on the following Lagrangian:

$$\begin{aligned}\mathcal{L} = & -y_{0LD}^{ij}\bar{\psi}_L^{0i}\phi_L D_R^j - y_{0LU}^{ij}\bar{\psi}_L^{0i}\tilde{\phi}_L U_R^j - y_{0RD}^{ij}\bar{\psi}_R^{0i}\phi_R D_L^j - y_{0RU}^{ij}\bar{\psi}_R^{0i}\tilde{\phi}_R U_L^j + (h.c.) \\ & -y_{0LE}^{ij}\bar{L}_L^{0i}\phi_L E_R^j - y_{0RE}^{ij}\bar{L}_R^{0i}\phi_R E_L^j + h.c. \\ & -\bar{U}^i M_{\mathcal{U}}^i U^i - \bar{D}^i M_{\mathcal{D}}^i D^i - \bar{E}^i M_{\mathcal{E}}^i E^i,\end{aligned}\tag{10}$$

where $M_{\mathcal{U}}^i, M_{\mathcal{D}}^i$ and $M_{\mathcal{E}}^i$ are real parameters. The representations under the gauge groups of ordinary quarks and charged leptons are assigned as:

$$\begin{aligned}\psi_L^{0i} &= \begin{pmatrix} u_0^i \\ d_0^i \end{pmatrix}_L : (2, 1, 1/3), & L_L^{0i} &= \begin{pmatrix} \nu_0^i \\ e_0^i \end{pmatrix}_L : (2, 1, -1), \\ \psi_R^{0i} &= \begin{pmatrix} u_0^i \\ d_0^i \end{pmatrix}_R : (1, 2, 1/3), & L_R^{0i} &= \begin{pmatrix} \nu_0^i \\ e_0^i \end{pmatrix}_R : (1, 2, -1), \\ U_{L,R}^i &: (1, 1, 4/3), & D_{L,R}^i &: (1, 1, -2/3), & E_{L,R}^i &: (1, 1, -2).\end{aligned}\tag{11}$$

We do not introduce singlet neutrinos and so there are no tree level neutrino masses. Let us first study the charged lepton sector and the down quark sector. The masses of the charged leptons and down quarks are much smaller than $O(100\text{GeV})$, so they can be treated in a unified way. We consider first the down-like quarks. In order to find the mixing angles (CKM matrix) among both left and right chiralities, it is convenient to perform unitary transformations among the ordinary quark fields such that the singlet-doublet Yukawa couplings, i.e. y_{0L} and y_{0R} , become triangular matrices [9],

$$U^\dagger y_0 = \begin{pmatrix} y_1 & 0 & 0 \\ y_{21} & y_2 & 0 \\ y_{31} & y_{32} & y_3 \end{pmatrix},\tag{12}$$

where U is a unitary matrix. The diagonal elements in Eq.(12) are real and the off-diagonal entries are complex. We perform this same type of transformation in the charged lepton sector. Accordingly, we obtain new bases for the $SU(2)$ doublet quarks and leptons,

$$\begin{aligned}u'_L &= U_{UL}^\dagger u_{0L}, & u'_R &= U_{RU}^\dagger u_{0R}, \\ d'_L &= U_{DL}^\dagger d_{0L}, & d'_R &= U_{DR}^\dagger d_{0R}, \\ e'_L &= U_{EL}^\dagger e_{0L}, & e'_R &= U_{ER}^\dagger e_{0R}, \\ \nu'_L &= U_{EL}^\dagger \nu_{0L}, & \nu'_R &= U_{ER}^\dagger \nu_{0R}.\end{aligned}\tag{13}$$

We note that the transformation on neutrinos is chosen to be the same as that on charged leptons. As a result, the down quark and charged lepton mass matrices are written as follows:

$$\mathcal{M}_{\mathcal{D}} = \begin{bmatrix} 0 & 0 & 0 & y_{LD1}\eta_L & 0 & 0 \\ 0 & 0 & 0 & y_{LD2}\eta_L & y_{LD2}\eta_L & 0 \\ 0 & 0 & 0 & y_{LD3}\eta_L & y_{LD32}\eta_L & y_{LD3}\eta_L \\ y_{RD1}\eta_R & y_{RD21}^*\eta_R & y_{RD31}^*\eta_R & M_D & 0 & 0 \\ 0 & y_{RD2}\eta_R & y_{RD32}^*\eta_R & 0 & M_S & 0 \\ 0 & 0 & y_{RD3}\eta_R & 0 & 0 & M_B \end{bmatrix}, \quad (14)$$

$$\mathcal{M}_{\mathcal{E}} = \begin{bmatrix} 0 & 0 & 0 & y_{LE1}\eta_L & 0 & 0 \\ 0 & 0 & 0 & y_{LE2}\eta_L & y_{LE2}\eta_L & 0 \\ 0 & 0 & 0 & y_{LE3}\eta_L & y_{LE32}\eta_L & y_{LE3}\eta_L \\ y_{RE1}\eta_R & y_{RE21}^*\eta_R & y_{RE31}^*\eta_R & M_E & 0 & 0 \\ 0 & y_{RE2}\eta_R & y_{RE32}^*\eta_R & 0 & M_\mu & 0 \\ 0 & 0 & y_{RE3}\eta_R & 0 & 0 & M_\tau \end{bmatrix}. \quad (15)$$

These mass matrices can be approximately diagonalized by using the following unitary matrices,

$$\begin{aligned} V_{0DL} &= \begin{pmatrix} 1 & y_{LD}\eta_L/M_{\mathcal{D}} \\ -1/M_{\mathcal{D}}y_{LD}^\dagger\eta_L & 1 \end{pmatrix}, \\ V_{0DR} &= \begin{pmatrix} 1 & y_{RD}\eta_R/M_{\mathcal{D}} \\ -1/M_{\mathcal{D}}y_{RD}^\dagger\eta_R & 1 \end{pmatrix}, \end{aligned} \quad (16)$$

where $M = \text{diag}(M_D, M_S, M_B)$. As a result, $\mathcal{M}_{\mathcal{D}}$ is approximately diagonalized as

$$V_{0DL}^\dagger \mathcal{M}_{\mathcal{D}} V_{0DR} \simeq \begin{pmatrix} -y_{LD1} \frac{\eta_L \eta_R}{M_D} y_{RD1} & -y_{LD1} \frac{\eta_L \eta_R}{M_D} y_{RD21}^* & -y_{LD1} \frac{\eta_L \eta_R}{M_D} y_{RD31}^* & 0 & 0 & 0 \\ -y_{LD21} \frac{\eta_L \eta_R}{M_D} y_{RD1} & -y_{LD2} \frac{\eta_L \eta_R}{M_S} y_{RD2} & -y_{LD2} \frac{\eta_L \eta_R}{M_S} y_{RD32}^* & 0 & 0 & 0 \\ -y_{LD31} \frac{\eta_L \eta_R}{M_D} y_{RD1} & -y_{LD32} \frac{\eta_L \eta_R}{M_S} y_{RD2} & -y_{LD3} \frac{\eta_L \eta_R}{M_B} y_{RD3} & 0 & 0 & 0 \\ 0 & 0 & 0 & M_D & 0 & 0 \\ 0 & 0 & 0 & 0 & M_S & 0 \\ 0 & 0 & 0 & 0 & 0 & M_B \end{pmatrix}. \quad (17)$$

Approximate eigenvalues of the down quark masses are given by the diagonal elements of Eq.(17) as:

$$\begin{aligned} m_b &\cong \frac{\eta_R}{M_B} y_{LD3} y_{RD3} \eta_L, \\ m_s &\cong \frac{\eta_R}{M_S} y_{RD2} y_{LD2} \eta_L, \\ m_d &\cong \frac{\eta_R}{M_D} y_{RD1} y_{LD1} \eta_L, \\ m_D &\cong M_D, \\ m_S &\cong M_S, \\ m_B &\cong M_B. \end{aligned} \quad (18)$$

For charged leptons, similar results are obtained.

3.1 Top quark mass and hierarchy of up type quark masses

Now we turn to the up type quark masses. In the previous section we saw that the top quark mass, in the absence of flavor mixing, is given by Eq.(9), rather than the seesaw type formula. The extension to the case where flavor mixing is present, and M_T is not exactly zero, but restricted to $M_T \ll \eta_R$, was done in [9]. Here we extend this previous analysis in a way that can be applied to the case where M_T is as large as η_R . First we derive the formulae for the top quark mass as well as the other light quark masses by solving the eigenvalue equation. Consider the up mass matrix:

$$\mathcal{M}_U = \begin{pmatrix} 0 & \eta_L y_{0LU} \\ \eta_R y_{0RU}^\dagger & M_U \end{pmatrix}, \quad (19)$$

where $M_U = \text{diag}(M_U, M_C, M_T)$. The corresponding eigenvalue equation for the quark masses is given by

$$\det(\mathcal{M}_U \mathcal{M}_U^\dagger - \Lambda) = \det \begin{bmatrix} \eta_L^2 y_{0LU} y_{0LU}^\dagger - \Lambda & y_{0LU} M_U \eta_L \\ \eta_L M_U y_{0LU}^\dagger & \eta_R^2 y_{0RU}^\dagger y_{0RU} + M_U^2 - \Lambda \end{bmatrix} = 0. \quad (20)$$

The equation which determines the eigenvalues of the order of η_L^2 (or smaller than η_L^2) is reduced to a cubic equation:

$$\det \left[y_{0LU} \left\{ 1 - M_U (\eta_R^2 y_{0RU}^\dagger y_{0RU} + M_U^2)^{-1} M_U \right\} y_{0LU}^\dagger - \lambda \right] = 0, \quad (21)$$

where we use the normalized eigenvalue $\lambda = \frac{\Lambda}{\eta_L^2}$. We further use the following expansion:

$$(\eta_R^2 y_{0RU}^\dagger y_{0RU} + M_U^2)^{-1} = \frac{1}{M_0} \left[1 - \left(\frac{1}{M_0} \Delta M^2 \frac{1}{M_0} \right) + \left(\frac{1}{M_0} \Delta M^2 \frac{1}{M_0} \right)^2 + \dots \right] \frac{1}{M_0}, \quad (22)$$

$$M_0 = \begin{bmatrix} M_U & & \\ & M_C & \\ & & \sqrt{\eta_R^2 (y_{0RU}^\dagger y_{0RU})_{33} + M_T^2} \end{bmatrix}. \quad (23)$$

Note that in the traditional treatment of the seesaw model, Eq.(22) is expanded by the inverse power of the singlet quark mass matrix, i.e., $\text{diag}(M_U, M_C, M_T)$. However the smallness of M_T compared with η_R does not allow us to do so. M_0 is chosen in such a way that the expansion by the inverse power of M_0 is still regular even in the limit of vanishing M_T . By keeping the dominant coefficients of $\lambda^n (n = 0, 1, 2, 3)$, the eigenvalue equation becomes,

$$\begin{aligned} F(\lambda) &= -\lambda^3 + \{\mathcal{L}_{33} \mathcal{R}_{33} X_T^2\} \lambda^2 \\ &- \{\mathcal{L}_{33} \mathcal{R}_{33} (\mathcal{L}_{22} - \mathcal{L}_{23} \mathcal{L}_{32} / \mathcal{L}_{33}) (\mathcal{R}_{22} - \mathcal{R}_{23} \mathcal{R}_{32} / \mathcal{R}_{33}) X_T^2 X_C^2\} \lambda \\ &+ X_T^2 X_C^2 X_U^2 \det \mathcal{L} \det \mathcal{R} = 0, \end{aligned} \quad (24)$$

where $\mathcal{L}_{ij} = (y_{0LU}^\dagger y_{0LU})_{ij}$, $\mathcal{R}_{ij} = (y_{0RU}^\dagger y_{0RU})_{ij}$, $X_U = \frac{\eta_R}{M_U}$, $X_C = \frac{\eta_R}{M_C}$, and $X_T = \frac{\eta_R}{\sqrt{M_T^2 + \mathcal{R}_{33}\eta_R^2}}$. By noting that $X_U \ll X_C \ll X_T = O(1)$, the approximate solution of Eq.(24) is

$$\begin{aligned} m_t &= \sqrt{\mathcal{L}_{33}\mathcal{R}_{33}} \frac{\eta_L\eta_R}{\sqrt{M_T^2 + \mathcal{R}_{33}\eta_R^2}}, \\ m_c &= \sqrt{(\mathcal{L}_{22} - \mathcal{L}_{23}\mathcal{L}_{32}/\mathcal{L}_{33})(\mathcal{R}_{22} - \mathcal{R}_{23}\mathcal{R}_{32}/\mathcal{R}_{33})} \left\{ \frac{\eta_L\eta_R}{M_C} \right\}, \\ m_u &= \sqrt{\frac{\det\mathcal{L} \det\mathcal{R}}{(\mathcal{L}_{22} - \mathcal{L}_{23}\mathcal{L}_{32}/\mathcal{L}_{33})(\mathcal{R}_{22} - \mathcal{R}_{23}\mathcal{R}_{32}/\mathcal{R}_{33})\mathcal{L}_{33}\mathcal{R}_{33}}} \left\{ \frac{\eta_L\eta_R}{M_U} \right\}. \end{aligned} \quad (25)$$

The heavier eigenvalues are also obtained as follows:

$$\begin{aligned} m_U &= M_U, \\ m_C &= M_C, \\ m_T &= \sqrt{M_T^2 + \mathcal{R}_{33}\eta_R^2}. \end{aligned} \quad (26)$$

To compare Eq.(25) and Eq.(26) with the formulae obtained in the absence of flavor mixing, Eq.(9), we need to explain a little bit more. The mass formulae for the light quarks are obtained in a weak basis in which the singlet quark mass matrix M is diagonal, and the singlet-doublet Yukawa couplings are general. However, the formulae are simplified if we go to the weak basis in which the singlet-doublet Yukawa couplings are in the triangular form. For example,

$$\begin{aligned} \sqrt{\mathcal{L}_{33}} &= y_{LU3}, \quad \sqrt{\mathcal{R}_{33}} = y_{RU3}, \\ \sqrt{\mathcal{L}_{22} - \mathcal{L}_{23}\mathcal{L}_{32}/\mathcal{L}_{33}} &= y_{LU2}, \quad \sqrt{\mathcal{R}_{22} - \mathcal{R}_{23}\mathcal{R}_{32}/\mathcal{R}_{33}} = y_{RU2}, \\ \sqrt{\det\mathcal{L}} &= (y_{LU1})(y_{LU2})(y_{LU3}), \quad \sqrt{\det\mathcal{R}} = (y_{RU1})(y_{RU2})(y_{RU3}). \end{aligned} \quad (27)$$

In this basis, the light quark masses are determined by the diagonal elements of the singlet-doublet Yukawa coupling:

$$\begin{aligned} m_t &= (y_{LU3})(y_{RU3}) \frac{\eta_L\eta_R}{\sqrt{M_T^2 + y_{RU3}^2\eta_R^2}}, \\ m_c &= (y_{LU2})(y_{RU2}) \left\{ \frac{\eta_L\eta_R}{M_C} \right\}, \\ m_u &= (y_{LU1})(y_{RU1}) \left\{ \frac{\eta_L\eta_R}{M_U} \right\}. \end{aligned} \quad (28)$$

The top quark mass in Eq.(28) reduces to the result obtained in Eq.(9). Therefore, we conclude that in the triangular basis, the off-diagonal elements of y_L and y_R can be safely neglected, since ignoring them does not affect the mass eigenvalues significantly. In the following section, it is shown that they are related to the size of the FCNC. Finally, we check the formulae Eq.(26) and Eq.(28) by showing that $\det\mathcal{M}_U = m_u m_c m_t m_U m_C m_T$. In fact, $\det\mathcal{M}_U$ is given by,

$$\begin{aligned} \det\mathcal{M}_U &= \sum_p \text{sign}(p) \mathcal{M}_{U1P(1)} \mathcal{M}_{U2P(2)} \mathcal{M}_{U3P(3)} \mathcal{M}_{U4P(4)} \mathcal{M}_{U5P(5)} \mathcal{M}_{U6P(6)} \\ &= \mathcal{M}_{U14} \mathcal{M}_{U25} \mathcal{M}_{U36} \mathcal{M}_{U41} \mathcal{M}_{U52} \mathcal{M}_{U63} \\ &= (y_{LU1})(y_{LU2})(y_{LU3})(y_{RU1})(y_{RU2})(y_{RU3})(\eta_L\eta_R)^6. \end{aligned} \quad (29)$$

With Eq.(26), Eq.(28) and $m_T = \sqrt{M_T^2 + y_{RU3}^2 \eta_R^2}$, $\det \mathcal{M}_U$ is equal to the products of mass eigenvalues of the six quarks.

4 Tree Level Z FCNC

In this section, we study the tree level FCNC due to neutral gauge boson exchange. We first derive the theoretical form of these flavor changing currents. This will show how they are naturally suppressed, and enable us to perform quantitative calculations. Using the estimates and the present experimental bounds on rare B and K decays, we examine whether the tree level FCNC can significantly contribute to them or not. We can also compare the tree level FCNC effects with one loop GIM suppressed contributions of the standard model.

Let us start with the relevant part of the Lagrangian:

$$\mathcal{L} = Z_1 J_1 + Z_2 J_2 + \frac{M_1^2 Z_1^2}{2} + \frac{M_2^2 Z_2^2}{2}, \quad (30)$$

where M_1 and M_2 are the mass eigenvalues of the neutral gauge boson mass matrix,

$$M^2 = M_{WR}^2 \begin{pmatrix} \frac{\cos^2 \theta_W}{\cos 2\theta_W} & 0 \\ 0 & 0 \end{pmatrix} + M_{WL}^2 \begin{pmatrix} \frac{\sin^2 \theta_W \tan^2 \theta_W}{\cos 2\theta_W} & \frac{\tan^2 \theta_W}{\sqrt{\cos 2\theta_W}} \\ \frac{\tan^2 \theta_W}{\sqrt{\cos 2\theta_W} \tan^2 \theta_W} & \frac{1}{\cos^2 \theta_W} \end{pmatrix}, \quad (31)$$

where M_{WR} and M_{WL} are masses of the charged SU(2) gauge bosons and $\sin \theta_W = e/g$ with SU(2) gauge coupling constant g and $U(1)_{em}$ gauge coupling constant e .

$$\begin{pmatrix} \cos \theta & \sin \theta \\ -\sin \theta & \cos \theta \end{pmatrix} M^2 \begin{pmatrix} \cos \theta & -\sin \theta \\ \sin \theta & \cos \theta \end{pmatrix} = \begin{pmatrix} M_2^2 & 0 \\ 0 & M_1^2 \end{pmatrix}. \quad (32)$$

When the breaking scale of $SU(2)_R$ is much larger than that of $SU(2)_L$, i.e. $M_{WR} \gg M_{WL}$, the eigenvalues and the mixing angle are approximately given by:

$$\begin{aligned} M_1^2 &= \frac{M_{WL}^2}{\cos^2 \theta_W} - \frac{M_{WL}^4 \tan^4 \theta_W}{M_{WR}^2 \cos^2 \theta_W}, \\ M_2^2 &= \frac{M_{WR}^2 \cos^2 \theta_W}{\cos 2\theta_W}, \\ \tan 2\theta &= \frac{2\sqrt{\cos 2\theta_W}}{\cos^2 \theta_W} \tan^2 \theta_W \frac{M_{WL}^2}{M_{WR}^2}, \end{aligned} \quad (33)$$

and J_1 and J_2 are written as:

$$\begin{aligned} J_1 &= J_1^0 \cos \theta - J_2^0 \sin \theta, \\ J_2 &= J_2^0 \cos \theta + J_1^0 \sin \theta, \\ J_1^0 &= \frac{g}{\cos \theta_W} (-J_{3L} + \sin^2 \theta_W J_Q), \\ J_2^0 &= g \frac{\cos \theta_W}{\sqrt{\cos 2\theta_W}} (-J_{3R} - \tan^2 \theta_W J_{3L} + \tan^2 \theta_W J_Q), \end{aligned} \quad (34)$$

where J_{3L} , J_{3R} , and J_Q are the $SU(2)_L$ isospin current, the $SU(2)_R$ isospin current, and the electromagnetic current, respectively. They are defined as:

$$J_{3L\mu} = \sum_{i=1}^3 \overline{\psi_L^{0i}} \gamma_\mu \frac{\tau_3}{2} \psi_L^{0i}, \quad J_{3R\mu} = \sum_{i=1}^3 \overline{\psi_R^{0i}} \gamma_\mu \frac{\tau_3}{2} \psi_R^{0i}, \quad J_{Q\mu} = \sum_{\alpha=1}^6 \overline{\psi^{0\alpha}} \gamma_\mu Q \psi^{0\alpha}. \quad (35)$$

We write the isospin currents in terms of the mass eigenstates,

$$d_L^{0i} = \sum_{\alpha=1}^6 V_{DL}^{i\alpha} d_L^\alpha, \quad d_R^{0i} = \sum_{\alpha=1}^6 V_{DR}^{i\alpha} d_R^\alpha, \quad (36)$$

where V_{DL} and V_{DR} are the 6×6 unitary matrices that diagonalize the seesaw type mass matrix,

$$V_{DL}^\dagger \begin{pmatrix} 0 & y_{0LD} \eta_L \\ y_{0RD}^\dagger \eta_R & M_D \end{pmatrix} V_{RD} = \begin{pmatrix} m_d & 0 \\ 0 & m_D \end{pmatrix}.$$

Now the neutral currents in the down quark sector are written as:

$$\begin{aligned} J_{3L} &= -\frac{1}{2} \sum_{\alpha\beta} \mathcal{Z}_{DL\alpha\beta} \overline{d_L^\alpha} \gamma_\mu d_L^\beta, \\ J_{3R} &= -\frac{1}{2} \sum_{\alpha\beta} \mathcal{Z}_{DR\alpha\beta} \overline{d_R^\alpha} \gamma_\mu d_R^\beta, \end{aligned} \quad (37)$$

where

$$\begin{aligned} \mathcal{Z}_{DL\alpha\beta} &= \sum_{i=1}^3 V_{DL}^{\dagger\alpha i} V_{DL}^{i\beta} = \delta^{\alpha\beta} - \sum_{I=4}^6 V_{DL}^{\dagger\alpha I} V_{DL}^{I\beta}, \\ \mathcal{Z}_{DR\alpha\beta} &= \sum_{i=1}^3 V_{DR}^{\dagger\alpha i} V_{DR}^{i\beta} = \delta^{\alpha\beta} - \sum_{I=4}^6 V_{DR}^{\dagger\alpha I} V_{DR}^{I\beta}. \end{aligned} \quad (38)$$

In this way the tree level exchange of neutral gauge bosons gives rise to the effective $\Delta F = 1$ Lagrangian,

$$\begin{aligned} \mathcal{L}^{\Delta F=1} &= \sqrt{2} G_F \sum_{\alpha \neq \beta} \{ \mathcal{Z}_{DL\alpha\beta} \overline{d_L^\alpha} \gamma_\mu d_L^\beta \overline{\nu_L^i} \gamma^\mu \nu_L^i + \beta \mathcal{Z}_{DR\alpha\beta} \overline{d_R^\alpha} \gamma_\mu d_R^\beta \overline{\nu_R^i} \gamma^\mu \nu_R^i \} \\ &- \sqrt{2} G_F \sum_{\alpha \neq \beta} \{ \mathcal{Z}_{DL\alpha\beta} \overline{d_L^\alpha} \gamma_\mu d_L^\beta (\overline{l_L^i} \gamma^\mu l_L^i - 2 \sin^2 \theta_W \overline{l^i} \gamma^\mu l^i) \\ &+ \beta \mathcal{Z}_{DR\alpha\beta} \overline{d_R^\alpha} \gamma_\mu d_R^\beta (\overline{l_R^i} \gamma^\mu l_R^i - 2 \sin^2 \theta_W \overline{l^i} \gamma^\mu l^i) \}, \end{aligned} \quad (39)$$

where the coefficient β is defined as $\beta = M_{W_L}^2 / M_{W_R}^2$. As we discuss below, the strength of the tree level FCNC couplings \mathcal{Z}_{DR} are enhanced by a factor of $1/\beta$ compared to \mathcal{Z}_{DL} . Therefore the $\Delta F = 1$ FCNC due to Z_1 is of the same order of magnitude as that of Z_2 .

We now turn to theoretical estimate. We first show how the FCNC among the ordinary down type quarks is suppressed. It turns out that the suppression factor is $m_d^i m_d^j / M_{W_R}^2$ for \mathcal{Z}_{DL}

and $m_d^i m_d^j / M_{W_L}^2$ for \mathcal{Z}_{DR} . As seen in Eq.(39), the FCNC couplings among the ordinary quarks are given by:

$$\begin{aligned}\mathcal{Z}_{DLij} &= -V_{DL}^{\dagger iI} V_{DL}^{Ij}, \\ \mathcal{Z}_{DRij} &= -V_{DR}^{\dagger iI} V_{DR}^{Ij}.\end{aligned}\quad (40)$$

In order to estimate the FCNC using Eq.(40), we must know V_{DL} and V_{DR} . For this purpose we can start with an approximate parameterization obtained from the diagonalization of the seesaw mass matrix and unitarity (see Eq.(12) and Eq.(13)), then we get

$$\begin{aligned}V_{DL} &= \begin{pmatrix} U_{DL} & 0 \\ 0 & 1 \end{pmatrix} V_{0DL} = \begin{pmatrix} U_{DL} & y_{0LD}\eta_L/M_{\mathcal{D}} \\ -1/M_{\mathcal{D}}y_{0LD}^\dagger\eta_L U_{DL} & 1 \end{pmatrix}, \\ V_{DR} &= \begin{pmatrix} U_{DR} & 0 \\ 0 & 1 \end{pmatrix} V_{0DR} = \begin{pmatrix} U_{DR} & y_{0RD}\eta_R/M_{\mathcal{D}} \\ -1/M_{\mathcal{D}}y_{0RD}^\dagger\eta_R U_{DR} & 1 \end{pmatrix},\end{aligned}\quad (41)$$

where U_{DL} and U_{DR} are unitary matrices that approximately diagonalize the 3×3 effective light quark mass matrix:

$$-U_{DL}^\dagger \left(y_{0LD} \frac{\eta_L \eta_R}{M_{\mathcal{D}}} y_{0RD}^\dagger \right) U_{DR} = m_d. \quad (42)$$

Notice that with a suitable choice of the unitary matrix U , an arbitrary matrix y_0 can be transformed into a triangular matrix, as in Eq.(12). Suppose $U_{DL}^\dagger y_{0DL}$ and $U_{DR}^\dagger y_{0DR}$ are such triangular matrices. We immediately find that the effective light quark mass matrix is approximately diagonalized,

$$-U_{DL}^\dagger \left(y_{0LD} \frac{\eta_L \eta_R}{M_{\mathcal{D}}} y_{0RD}^\dagger \right) U_{DR} = - \begin{pmatrix} y_{DL1} \frac{1}{M_D} y_{DR1} & y_{DL1} \frac{1}{M_D} y_{DR2}^* & y_{DL1} \frac{1}{M_D} y_{DR3}^* \\ y_{DL21} \frac{1}{M_D} y_{DR1} & y_{DL2} \frac{1}{M_S} y_{DR2} & y_{DL2} \frac{1}{M_S} y_{DR3}^* \\ y_{DL31} \frac{1}{M_D} y_{DR1} & y_{DL32} \frac{1}{M_S} y_{DR2} & y_{DL3} \frac{1}{M_B} y_{DR3} \end{pmatrix} \eta_L \eta_R, \quad (43)$$

where we assume the following hierarchy of the singlet quark masses,

$$M_D \gg M_S \gg M_B. \quad (44)$$

Therefore the light quark masses are approximately given by the diagonal elements of Eq.(43),

$$m_d^i = - \left(y_{DLi} \frac{1}{M_{\mathcal{D}i}} y_{DRi} \right) \eta_L \eta_R. \quad (45)$$

Substituting the approximate parameterization of V_{DL} and V_{DR} into Eq.(41), we obtain the following formulae for the FCNC:

$$\begin{aligned}\mathcal{Z}_{DL}^{ij} &= -\{U_{DL}^\dagger y_{0LD} \frac{\eta_L^2}{M_{\mathcal{D}}^2} y_{0LD}^\dagger U_{DL}\}_{ij} \\ &= -m_d^i \{U_{DR}^\dagger y_{0RD} y_{0RD}^\dagger U_{DR}\}^{-1}_{ij} m_d^j / \eta_R^2, \\ \mathcal{Z}_{DR}^{ij} &= -m_d^i \{U_{DL}^\dagger y_{0LD} y_{0LD}^\dagger U_{DL}\}^{-1}_{ij} m_d^j / \eta_L^2.\end{aligned}\quad (46)$$

We must check that the right hand side does not necessarily vanish when $i \neq j$. We can see that this is indeed the case because $U_L^\dagger y_{0L}$ and $U_R^\dagger y_{0R}$ are triangular matrices, and their off diagonal elements, y_{ijL} and y_{ijR} ($i \neq j$), are non-zero in general. To leading order the off diagonal elements are given by:

$$\begin{aligned} \{U_{DR}^\dagger y_{0RD} y_{0RD}^\dagger U_{DR}\}_{ij}^{-1} &\simeq \begin{cases} -\frac{y_{RDji}^*}{y_{RDj} y_{RDj}^2} & (i < j), \\ -\frac{y_{RDij}}{y_{RDj} y_{RDj}^2} & (i > j), \end{cases} \\ \{U_{DL}^\dagger y_{0LD} y_{0LD}^\dagger U_{DL}\}_{ij}^{-1} &\simeq \begin{cases} -\frac{y_{DLji}^*}{y_{LDi} y_{LDj}^2} & (i < j), \\ -\frac{y_{DLij}}{y_{LDj} y_{LDj}^2} & (i > j), \end{cases} \end{aligned} \quad (47)$$

so the FCNC couplings are suppressed as:

$$\begin{aligned} \mathcal{Z}_{DLij} &= -\{m_d^i m_d^j / 2M_{W_R}^2\} g^2 (U_{DR}^\dagger y_{RD} y_{RD}^\dagger U_{DR})_{ij}^{-1} \\ &\simeq (m_d^i m_d^j / 2M_{W_R}^2) \frac{y_{RDji}^*}{y_{RDj}} \left(\frac{g}{y_{RDj}}\right)^2 \quad (i < j), \\ \mathcal{Z}_{DLij} &= \mathcal{Z}_{DLji}^* \quad (i > j), \\ \mathcal{Z}_{DRij} &= -\{m_d^i m_d^j / 2M_{W_L}^2\} g^2 (U_{DL}^\dagger y_{LD} y_{LD}^\dagger U_{DL})_{ij}^{-1} \\ &\simeq (m_d^i m_d^j / 2M_{W_L}^2) \frac{y_{LDji}^*}{y_{LDi}} \left(\frac{g}{y_{LDj}}\right)^2 \quad (i < j), \\ \mathcal{Z}_{DRij} &= \mathcal{Z}_{DRji}^* \quad (i > j). \end{aligned} \quad (48)$$

Therefore the tree level FCNC among the light quarks is naturally suppressed by a factor of $(\text{quark masses})^2$ divided by an $(SU(2) \text{ breaking scale})^2$. Also, they are proportional to the off-diagonal elements of y_{ij} . If all of these vanish, there are no FCNC among light quarks.

We can now confront our result for the FCNC with the present experimental bounds from rare K and B decays.

$$\begin{aligned} \mathcal{Z}_{Rsd} &\simeq \frac{m_s m_d}{2M_{W_L}^2} \frac{y_{Lsd}}{y_{Ld}} \left(\frac{g}{y_{Ls}}\right)^2 = 3.1 \times 10^{-7} \left\{ \frac{y_{Lsd}}{2y_{Ld}} \left(\frac{g}{y_{Ls}}\right)^2 \right\}, \\ \mathcal{Z}_{Rbd} &\simeq \frac{m_b m_d}{2M_{W_L}^2} \frac{y_{Lbd}}{y_{Ld}} \left(\frac{g}{y_{Lb}}\right)^2 = 7.8 \times 10^{-6} \left\{ \frac{y_{Lbd}}{2y_{Ld}} \left(\frac{g}{y_{Lb}}\right)^2 \right\}, \\ \mathcal{Z}_{Rbs} &\simeq \frac{m_b m_s}{2M_{W_L}^2} \frac{y_{Lbs}}{y_{Ls}} \left(\frac{g}{y_{Lb}}\right)^2 = 1.6 \times 10^{-4} \left\{ \frac{y_{Lbs}}{2y_{Ls}} \left(\frac{g}{y_{Lb}}\right)^2 \right\}, \\ \mathcal{Z}_{Lsd} &\simeq \beta \frac{m_s m_d}{2M_{W_R}^2} \frac{y_{Rsd}}{y_{Rd}} \left(\frac{g}{y_{Rs}}\right)^2 = 1.2 \times 10^{-8} \left(\frac{400}{M_{W_R}(GeV)}\right)^2 \left\{ \frac{y_{Rsd}}{2y_{Rd}} \left(\frac{g}{y_{Rs}}\right)^2 \right\}, \\ \mathcal{Z}_{Lbd} &\simeq \beta \frac{m_b m_d}{2M_{W_R}^2} \frac{y_{Rbd}}{y_{Rd}} \left(\frac{g}{y_{Rb}}\right)^2 = 3.1 \times 10^{-7} \left(\frac{400}{M_{W_R}(GeV)}\right)^2 \left\{ \frac{y_{Rbd}}{2y_{Rd}} \left(\frac{g}{y_{Rb}}\right)^2 \right\}, \\ \mathcal{Z}_{Lbs} &\simeq \beta \frac{m_b m_s}{2M_{W_R}^2} \frac{y_{Rbs}}{y_{Rs}} \left(\frac{g}{y_{Rb}}\right)^2 = 6.4 \times 10^{-6} \left(\frac{400}{M_{W_R}(GeV)}\right)^2 \left\{ \frac{y_{Rbs}}{2y_{Rs}} \left(\frac{g}{y_{Rb}}\right)^2 \right\}, \end{aligned}$$

$$\beta = \frac{M_{WL}^2}{M_{WR}^2}, \quad (49)$$

where we use $m_d = 10$ MeV, $m_s = 0.2$ GeV, $m_b = 5$ GeV and $M_{WL} = 80$ GeV. We also use the following notations. $\mathcal{Z}_{Lbs} \equiv \mathcal{Z}_{DL32}$, $y_{Rbs} \equiv y_{RD32}$ and so on. The tree level contribution to the branching ratio $B \rightarrow X_s e^+ e^-$ and $K^+ \rightarrow \pi^+ \nu \bar{\nu}$ is given by,

$$\frac{\mathcal{B}(K^+ \rightarrow \pi^+ \nu \bar{\nu})|_{\text{Tree}}}{\mathcal{B}(K^+ \rightarrow \pi^0 e^+ \nu)} = \frac{3}{2} \frac{|\mathcal{Z}_{Lsd}|^2 + \beta^2 |\mathcal{Z}_{Rsd}|^2}{|V_{us}|^2}, \quad (50)$$

$$\frac{\mathcal{B}(B \rightarrow X_s e^+ e^-)|_{\text{Tree}}}{\mathcal{B}(B \rightarrow X_c l^- \bar{\nu})} = \frac{P_s}{P_c} \frac{1}{4} \{ (1 - 2 \sin^2 \theta_W)^2 + 4 \sin^4 \theta_W \} \frac{|\mathcal{Z}_{Lsb}|^2 + \beta^2 |\mathcal{Z}_{Rsb}|^2}{|V_{cb}|^2}, \quad (51)$$

where $P_c = 0.538$ and $P_s = 0.986$ are the phase space factors for the charm quark and the strange quark, respectively. Using $\mathcal{B}(B \rightarrow X_c l^- \bar{\nu}) \simeq 10\%$, $|V_{cb}^{\text{CKM}}| = 0.04$, $\mathcal{B}(K^+ \rightarrow \pi^0 e^+ \nu) \simeq 5\%$ and $|V_{us}^{\text{CKM}}| = 0.22$ [12], the order of the magnitude of the tree level contribution to these processes are,

$$\begin{aligned} \mathcal{B}(B \rightarrow X_s e^+ e^-)|_{\text{Tree}} &\leq 1.4 \times 10^{-9}, \\ \mathcal{B}(K^+ \rightarrow \pi^+ \nu \bar{\nu})|_{\text{Tree}} &\leq 4.5 \times 10^{-16}, \end{aligned} \quad (52)$$

where $M_{WR} \geq 400(\text{GeV})$ and the combination of the coefficient of Yukawa coupling and gauge coupling in Eq.(49) is set to be $\mathcal{O}(1)$. The experimental bound [13] and the prediction of the standard model [14] of $B \rightarrow X_s e^+ e^-$ are,

$$\begin{aligned} \mathcal{B}(B \rightarrow X_s e^+ e^-)|_{\text{Exp.}} &\leq 5.7 \times 10^{-5}, \\ \mathcal{B}(B \rightarrow X_s e^+ e^-)|_{\text{SM}} &\simeq 8.4 \pm 2.3 \times 10^{-6}, \end{aligned} \quad (53)$$

while the recent measurement of $K^+ \rightarrow \pi^+ \nu \bar{\nu}$ [15] and the prediction of the standard model [18] are given by,

$$\begin{aligned} \mathcal{B}(K^+ \rightarrow \pi^+ \nu \bar{\nu})|_{\text{Exp.}} &= 4.2_{-3.5}^{+9.7} \times 10^{-10}, \\ \mathcal{B}(K^+ \rightarrow \pi^+ \nu \bar{\nu})|_{\text{SM}} &= 0.6 \sim 1.5 \times 10^{-10}. \end{aligned} \quad (54)$$

Compared with values in Eqs.(52), (53) and (54), the tree level FCNC is found to be negligibly small. In section 6 and 7, we investigate the FCNC in one-loop level.

5 The flavor mixing in the charged currents

In this section, we present the approximate parameterization of the flavor mixing in the charged currents which is analogous to CKM matrix in the standard model (SM). The difference between the CKM in the standard model and that of the present model is that the flavor mixing in the present model is 6×6 rather than 3×3 in the SM. There is also right-handed flavor mixing in the present model. As we show in the following, the flavor mixing consists of the singlet-doublet

mixing and the flavor mixing among doublet quarks. The charged currents of the present model are written as,

$$\begin{aligned} J_{L\mu} &= \overline{u_L^\alpha} \gamma_\mu V_{\alpha\beta}^L d_L^\beta, \\ J_{R\mu} &= \overline{u_R^\alpha} \gamma_\mu V_{\alpha\beta}^R d_R^\beta, \end{aligned} \quad (55)$$

where V^L and V^R are the generalized CKM matrix and are given by

$$\begin{aligned} V_{\alpha\beta}^L &= \sum_i^3 V_{UL\alpha i}^\dagger V_{DLi\beta} = \sum_i^3 V_{0UL\alpha i}^\dagger U_{ij}^L V_{0DLj\beta}, \\ V_{\alpha\beta}^R &= \sum_i^3 V_{UR\alpha i}^\dagger V_{DRi\beta} = \sum_i^3 V_{0UR\alpha i}^\dagger U_{ij}^R V_{0DRj\beta}, \end{aligned} \quad (56)$$

where U_{ij}^L and U_{ij}^R are 3 by 3 unitary matrices and are defined by,

$$\begin{aligned} U^L &= U_{UL}^\dagger U_{DL}, \\ U^R &= U_{UR}^\dagger U_{DR}. \end{aligned} \quad (57)$$

U_{UL}, U_{UR}, U_{DL} , and U_{DR} are 3×3 unitary matrices which transform the singlet-doublet Yukawa matrices $y_{0UL}, y_{0UR}, y_{0DL}$, and y_{0DR} into the triangular matrices, y_{UL}, y_{UR}, y_{DL} , and y_{DR} . $V_{0UL/R}(V_{0DL/R})$ are matrices which diagonalize $\mathcal{M}_{\mathcal{U}}$ and $\mathcal{M}_{\mathcal{D}}$ as,

$$\begin{aligned} V_{0UL}^\dagger \mathcal{M}_{\mathcal{U}} V_{0UR} &= \begin{pmatrix} m_u & 0 \\ 0 & m_U \end{pmatrix}, \\ V_{0DL}^\dagger \mathcal{M}_{\mathcal{D}} V_{0DR} &= \begin{pmatrix} m_d & 0 \\ 0 & m_D \end{pmatrix}, \end{aligned} \quad (58)$$

where

$$\begin{aligned} \mathcal{M}_{\mathcal{U}} &= \begin{pmatrix} 0 & y_{UL}\eta_L \\ y_{UR}^\dagger\eta_R & M_{\mathcal{U}} \end{pmatrix}, \\ \mathcal{M}_{\mathcal{D}} &= \begin{pmatrix} 0 & y_{DL}\eta_L \\ y_{DR}^\dagger\eta_R & M_{\mathcal{D}} \end{pmatrix}. \end{aligned} \quad (59)$$

Because the mass eigenvalues are not affected significantly by the presence of the off-diagonal element of the triangular matrices y_{UL}, y_{UR}, y_{DL} and y_{DR} , it is legitimate to neglect the off-diagonal element of the triangular matrices. In the approximation, $\mathcal{M}_{\mathcal{D}}$ and $\mathcal{M}_{\mathcal{U}}$ are approximated as,

$$\mathcal{M}_{\mathcal{U}} \simeq \begin{bmatrix} 0 & 0 & 0 & y_{LU1}\eta_L & 0 & 0 \\ 0 & 0 & 0 & 0 & y_{LU2}\eta_L & 0 \\ 0 & 0 & 0 & 0 & 0 & y_{LU3}\eta_L \\ y_{RU1}\eta_R & 0 & 0 & M_U & 0 & 0 \\ 0 & y_{RU2}\eta_R & 0 & 0 & M_C & 0 \\ 0 & 0 & y_{RU3}\eta_R & 0 & 0 & M_T \end{bmatrix},$$

$$\mathcal{M}_{\mathcal{D}} \simeq \begin{bmatrix} 0 & 0 & 0 & y_{LD1}\eta_L & 0 & 0 \\ 0 & 0 & 0 & 0 & y_{LD2}\eta_L & 0 \\ 0 & 0 & 0 & 0 & 0 & y_{LD3}\eta_L \\ y_{RD1}\eta_R & 0 & 0 & M_D & 0 & 0 \\ 0 & y_{RD2}\eta_R & 0 & 0 & M_S & 0 \\ 0 & 0 & y_{RD3}\eta_R & 0 & 0 & M_B \end{bmatrix}. \quad (60)$$

It may be useful to comment on the diagonal forms of the matrices in Eq.(60). These simple block-diagonal forms follow from neglecting the off diagonal entries of the initial 6×6 quark mass matrices as in Eq.(60). Therefore, the forms of Eq.(60) become more complex in general if the off diagonal entries of the triangular matrices denoted by y_L and y_R of the quark mass matrices are included. Because the tree level FCNC is already suppressed, in one loop level calculation, we can set $Z_{ij} = 0$. This is equivalent to neglecting the off-diagonal element of the triangular matrices y_{ij} in the one-loop calculation. Therefore, it is sufficient to keep only the diagonal element of y for the present purpose. In the approximation, there is a convenient parameterization of the 6×6 generalized KM. First the matrices shown in Eq.(60) can be diagonalized by the 2 by 2 block diagonal matrices, because we only need to diagonalize a singlet-doublet mixing in each flavor,

$$\begin{aligned} V_{0LU} &= \begin{pmatrix} C_{LU} & S_{LU} \\ -S_{LU} & C_{LU} \end{pmatrix}, & V_{0RU} &= \begin{pmatrix} C_{RU} & S_{RU} \\ -S_{RU} & C_{RU} \end{pmatrix}, \\ V_{0LD} &= \begin{pmatrix} C_{LD} & S_{LD} \\ -S_{LD} & C_{LD} \end{pmatrix}, & V_{0RD} &= \begin{pmatrix} C_{RD} & S_{RD} \\ -S_{RD} & C_{RD} \end{pmatrix}, \end{aligned} \quad (61)$$

where,

$$\begin{aligned} S_{LU} &= \begin{pmatrix} s_{Lu} & 0 & 0 \\ 0 & s_{Lc} & 0 \\ 0 & 0 & s_{Lt} \end{pmatrix}, & C_{LU} &= \begin{pmatrix} c_{Lu} & 0 & 0 \\ 0 & c_{Lc} & 0 \\ 0 & 0 & c_{Lt} \end{pmatrix}, \\ S_{RU} &= \begin{pmatrix} s_{Ru} & 0 & 0 \\ 0 & s_{Rc} & 0 \\ 0 & 0 & s_{Rt} \end{pmatrix}, & C_{RU} &= \begin{pmatrix} c_{Ru} & 0 & 0 \\ 0 & c_{Rc} & 0 \\ 0 & 0 & c_{Rt} \end{pmatrix}, \\ S_{LD} &= \begin{pmatrix} s_{Ld} & 0 & 0 \\ 0 & s_{Ls} & 0 \\ 0 & 0 & s_{Lb} \end{pmatrix}, & C_{LD} &= \begin{pmatrix} c_{Ld} & 0 & 0 \\ 0 & c_{Ls} & 0 \\ 0 & 0 & c_{Lb} \end{pmatrix}, \\ S_{RD} &= \begin{pmatrix} s_{Rd} & 0 & 0 \\ 0 & s_{Rs} & 0 \\ 0 & 0 & s_{Rb} \end{pmatrix}, & C_{RD} &= \begin{pmatrix} c_{Rd} & 0 & 0 \\ 0 & c_{Rs} & 0 \\ 0 & 0 & c_{Rb} \end{pmatrix}, \end{aligned} \quad (62)$$

with $s_{Lu} = \sin \theta_{Lu}$ and $c_{Lu} = \cos \theta_{Lu}$ etc. and likewise for the down-quark sector. The flavor mixings of left handed quarks are given by the following 6×6 matrix:

$$V^L = \begin{pmatrix} C_{LU} & -S_{LU} \\ S_{LU} & C_{LU} \end{pmatrix} \begin{pmatrix} U^L & 0 \\ 0 & 0 \end{pmatrix} \begin{pmatrix} C_{LD} & S_{LD} \\ -S_{LD} & C_{LD} \end{pmatrix} = \begin{pmatrix} C_{LU}U^LC_{LD} & C_{LU}U^LS_{LD} \\ S_{LU}U^LC_{LD} & S_{LU}U^LS_{LD} \end{pmatrix}, \quad (63)$$

where 3×3 part of the generalized KM matrix V^L is no longer unitary, while U^L is an unitary matrix. For the right-handed quarks, the CKM matrix is given as follows:

$$V^R = \begin{pmatrix} C_{RU}U^RC_{RD} & C_{RU}U^RS_{RD} \\ S_{RU}U^RC_{RD} & S_{RU}U^RS_{RD} \end{pmatrix}. \quad (64)$$

We give an approximate parameterization of V^L and V^R . We first note that the mixings s_{Li} and s_{Ri} are expressed in terms of the mass matrices elements:

$$s_{Lu} \simeq \frac{y_{LU1}\eta_L}{M_U}, \quad s_{Lc} \simeq \frac{y_{LU2}\eta_L}{M_C}, \quad s_{Lt} = \sin \left[\frac{1}{2} \tan^{-1} \frac{2|y_{LU3}|\eta_L M_T}{|y_{RU3}|^2\eta_R^2 + M_T^2 - |y_{LU3}|^2\eta_L^2} \right], \quad (65)$$

$$s_{Ru} \simeq \frac{y_{RU1}\eta_R}{M_U}, \quad s_{Rc} \simeq \frac{y_{RU2}\eta_R}{M_C}, \quad c_{Rt} = \sin \left[\frac{1}{2} \tan^{-1} \frac{2|y_{RU3}|\eta_R M_T}{|y_{RU3}|^2\eta_R^2 - M_T^2 - |y_{LU3}|^2\eta_L^2} \right]. \quad (66)$$

There is a simple relation among the mixing angles, the light quark mass m_{qi} and heavy quark mass m_{Qi} which follows from zeros of the 3×3 ordinary light quark sector of the mass matrix,

$$c_{Ri}c_{Li}m_{qi} = -s_{Ri}s_{Li}m_{Qi}. \quad (67)$$

These relations are useful to estimate the box contributions in FCNC. We observe the following facts on the mixing angles between the singlet and doublet quarks.

- The mixing angles are suppressed as $s_{Li} = O(m_i/M_{WR})$ and $s_{Ri} = O(m_i/M_{WL})$ for light five quarks (from up to bottom quarks) and their singlet partners.
- s_{Lt} is at the most $O(\frac{M_{WL}}{M_{WR}})$ with $M_T = O(\eta_R)$. For $M_{WR} > 400(GeV)$, s_{Lt} may be less than 0.2.
- s_{Rt} is not suppressed. In section 2, we argue that when $M_T < M_{WR}$, we can prevent the seesaw mechanism to act and the top quark mass is at the electroweak breaking scale without introducing non-perturbative Yukawa coupling. This corresponds to $c_{Rt} = O(\frac{M_T}{M_{WR}}) < 1$ and s_{Rt} is close to one.

Because U^L is 3×3 unitary matrix and we have direct measurements on V_{ui}^L and V_{ci}^L , we can parameterize U^L with the Wolfenstein parameterization. About the right-handed KM, we are guided by theoretical assumption. We assume that the Yukawa coupling between the doublet and the singlet quarks is left-right symmetric, $y_L = y_R$. This reduces to $U^L = U^R$. In the following section, we always assume this relation. It is instructive to write the generalized KM V^L and V^R explicitly in the approximate parameterization. We are interested in the charged currents between light down type quarks (d,s,b) and up type quarks. By neglecting the small mixings to the heavy quarks (U,D,S,B,C), 4×3 part of the V^L and V^R are:

$$\left(\bar{u}_L \bar{c}_L \bar{t}_L \bar{T}_L \right) \begin{pmatrix} 1 - \frac{\lambda^2}{2} & \lambda & A\lambda^3(\rho - i\eta) \\ -\lambda - iA^2\lambda^5\eta & 1 - \frac{\lambda^2}{2} & A\lambda^2 \\ c_{Lt}A\lambda^3(1 - \rho - i\eta) & c_{Lt}(-A - iA\lambda^4\eta)\lambda^2 & c_{Lt} \\ s_{Lt}A\lambda^3(1 - \rho - i\eta) & s_{Lt}(-A - iA\lambda^4\eta)\lambda^2 & s_{Lt} \end{pmatrix} \begin{pmatrix} d_L \\ s_L \\ b_L \end{pmatrix}, \quad (68)$$

$$\left(\begin{array}{c} \bar{u}_R \bar{c}_R \bar{t}_R \bar{T}_R \end{array} \right) \left(\begin{array}{ccc} 1 - \frac{\lambda^2}{2} & \lambda & A\lambda^3(\rho - i\eta) \\ -\lambda - iA^2\lambda^5\eta & 1 - \frac{\lambda^2}{2} & A\lambda^2 \\ c_{Rt}A\lambda^3(1 - \rho - i\eta) & c_{Rt}(-A\lambda^2 - iA\lambda^4\eta) & c_{Rt} \\ s_{Rt}A\lambda^3(1 - \rho - i\eta) & s_{Rt}(-A\lambda^2 - iA\lambda^4\eta) & s_{Rt} \end{array} \right) \left(\begin{array}{c} d_R \\ s_R \\ b_R \end{array} \right). \quad (69)$$

Note that V^L and V^R is not left-right symmetric. In the limit of $\frac{M_T}{M_{WR}} = 0$, they are given by,

$$V^L = \left(\begin{array}{ccc} 1 - \frac{\lambda^2}{2} & \lambda & A\lambda^3(\rho - i\eta) \\ -\lambda - iA^2\lambda^5\eta & 1 - \frac{\lambda^2}{2} & A\lambda^2 \\ A\lambda^3(1 - \rho - i\eta) & -A\lambda^2 - iA^2\lambda^4\eta & 1 \\ 0 & 0 & 0 \end{array} \right), \quad (70)$$

$$V^R = \left(\begin{array}{ccc} 1 - \frac{\lambda^2}{2} & \lambda & A\lambda^3(\rho - i\eta) \\ -\lambda - iA^2\lambda^5\eta & 1 - \frac{\lambda^2}{2} & A\lambda^2 \\ 0 & 0 & 0 \\ A\lambda^3(1 - \rho - i\eta) & -A\lambda^2 - iA\lambda^4\eta & 1 \end{array} \right). \quad (71)$$

6 One-Loop Level FCNC

In the present model, there are many particles which may contribute to the FCNC in the one-loop level. For example, there are new contributions to the $\Delta F = 2$ transition from box diagrams involving ordinary quarks and heavy isosinglet quark intermediate states. They can contribute to the Feynman diagrams in which $W_L W_L$, $W_L W_R$ and $W_R W_R$ are exchanged. $W_R W_R$ exchanged diagrams are suppressed and we ignore their effect. The major contribution from $W_L W_L$ and $W_R W_L$ exchanged diagrams is discussed below.

In the $W_L W_L$ exchanged diagrams, the lightest singlet up type quark T can contribute. We denote $M_{12}(SM)$ as the contribution to the off-diagonal matrix element of neutral meson systems, i.e., $K\bar{K}$ and $B\bar{B}$ in the SM. $M_{12}(LL)$ is the $W_L W_L$ exchanged box diagram in the present model in which T quark loop is taken account of. The deviation from the SM due to T quark loop can be written with Inami-Lim functions,

$$\begin{aligned} \frac{M_{12}(LL) - M_{12}(SM)}{M_{12}(SM)} &\simeq (\lambda_t^{LL})^2 \left(2 \left(\frac{S(x_t, x_T)}{S(x_t)} - 1 \right) s_{Lt}^2 c_{Lt}^2 + \left(\frac{S(x_T)}{S(x_t)} - 1 \right) s_{Lt}^4 \right), \\ \lambda_t^{LL} &= U_{tk}^{L*} U_{tl}^L, \quad (k, l) = (d, s), (d, b), (s, b), \\ x_t &= \left(\frac{m_t}{M_{WL}} \right)^2, \quad x_T = \left(\frac{m_T}{M_{WL}} \right)^2, \end{aligned} \quad (72)$$

where $(k, l) = (d, s), (d, b),$ and (s, b) correspond to $K\bar{K}$, $B_d\bar{B}_d$ and $B_s\bar{B}_s$ mixings respectively. $S(x)$ and $S(x, y)$ are the Inami-Lim functions. s_{Lt} is the mixing angle of the singlet quark T defined in Eq.(65). The mixing angle is approximately given by,

$$s_{Lt} = O\left(\frac{M_{WL} M_T}{M_{WR}^2}\right). \quad (73)$$

We find that for $M_T = O(M_{WL})$, the mixing angle is suppressed as $s_{Lt} = O(\frac{M_{WL}^2}{M_{WR}^2})$. For $M_T = O(M_{WR})$, we obtain the larger mixing angle, i.e., $s_{Lt} = O(\frac{M_{WL}}{M_{WR}})$. When $M_{WR} \simeq 400(\text{GeV})$, for the former case, the mixing angle is 0.04 and for the latter case, it is 0.2. Therefore, for the smaller $M_T = O(M_{WL})$, the T quark does not contribute to $W_L W_L$ exchanged diagrams at all. For the larger mixing angle case, the deviation from the SM can be as large as 30% for $M_{WR} \simeq 400\text{GeV}$. In the subsequent analysis, we extensively study the case for the small mixing angle. Then $W_L W_L$ box diagram contribution is not changed from that of the SM, i.e., $M_{12}(LL) \simeq M_{12}(SM)$. For the latter case, we need to do more careful analysis and this will be done in the future publication.

When the T quark contribution to $W_L W_L$ exchanged diagrams is small, the most important contribution comes from $W_R W_L$ exchanged diagrams. [19] In the $W_R W_L$ exchanged diagrams (Fig.1), we must also take account of both isosinglet and isodoublet quarks as intermediate states.

6.1 $K^0 - \bar{K}^0$ mixing

The $K^0 - \bar{K}^0$ mixing is one of the best processes to test the FCNC in our model. We reexamine the famous enhancement factor in $W_L - W_R$ box diagrams of LR models [19] taking account of both isosinglet and isodoublet quarks as intermediate states. The effective Hamiltonian for $W_L - W_R$ exchanged diagram is,

$$H_{\text{eff}}(LR) = \frac{G_F^2}{4\pi^2} M_{WL}^2 \Lambda_\gamma^{LR} \Lambda_\delta^{RL} 2\beta \sqrt{x_\gamma x_\delta} F(x_\gamma, x_\delta, \beta) (\bar{d}Ls)(\bar{d}Rs), \quad (74)$$

where

$$\Lambda_\gamma^{LR} = V_{q_\gamma d}^{L*} V_{q_\gamma s}^R, \quad \Lambda_\delta^{RL} = V_{q_\delta d}^{R*} V_{q_\delta s}^L, \quad q_{\gamma,\delta} = (u, c, t, U, C, T), \quad (75)$$

and

$$\beta = \left(\frac{M_{WL}}{M_{WR}} \right)^2, \quad F(x_\gamma, x_\delta, \beta) = (4 + \beta x_\gamma x_\delta) I_1(x_\gamma, x_\delta, \beta) - (1 + \beta) I_2(x_\gamma, x_\delta, \beta), \quad (76)$$

$$x_\gamma \equiv x_{q_i} = \left(\frac{m_{q_i}}{M_{WL}} \right)^2 \quad (\gamma = 1 \sim 3), \quad x_\gamma \equiv X_{Q_i} = \left(\frac{m_{Q_i}}{M_{WL}} \right)^2 \quad (\gamma = 4 \sim 6), \quad (77)$$

where i runs from 1 to 3 and $V^{L/R}$ denotes the 6×6 mixing matrices. The loop functions I_1 and I_2 are found to be the same ones given by Ecker and Grimus[20]:

$$I_1(x_\gamma, x_\delta, \beta) = \frac{x_\gamma \ln x_\gamma}{(1 - x_\gamma)(x_\gamma - x_\delta)(1 - \beta x_\gamma)} + (x_\gamma \leftrightarrow x_\delta) - \frac{\beta \ln \beta}{(1 - \beta x_\gamma)(1 - \beta x_\delta)(1 - \beta)}, \quad (78)$$

$$I_2(x_\gamma, x_\delta, \beta) = \frac{x_\gamma^2 \ln x_\gamma}{(1 - x_\gamma)(1 - \beta x_\gamma)(x_\gamma - x_\delta)} + (x_\gamma \leftrightarrow x_\delta) - \frac{\ln \beta}{(1 - \beta)(1 - \beta x_\gamma)(1 - \beta x_\delta)}. \quad (79)$$

The contribution to the off diagonal matrix element M_{12}^K is

$$M_{12}^K(LR) = \frac{G_F^2}{4\pi^2} M_{W_L}^2 \Lambda_\gamma^{LR} \Lambda_\delta^{RL} 2\beta \sqrt{x_\gamma x_\delta} F(x_\gamma, x_\delta, \beta) \langle K^0 | (\bar{d}Ls)(\bar{d}Rs) | \bar{K}^0 \rangle \frac{1}{2m_K}. \quad (80)$$

The K_L and K_S mass difference, Δm_K and the CP violating parameter ϵ_K are given:

$$\Delta m_K = 2\text{Re}M_{12}^K, \quad \epsilon_K = \exp(i\frac{\pi}{4}) \left(\frac{\text{Im}M_{12}^K}{\sqrt{2}\Delta m_K} + \xi_0 \right), \quad \xi_0 = \frac{\text{Im}A_0}{\text{Re}A_0}. \quad (81)$$

The LR contribution to Δm_K is given by

$$\Delta m_K(LR) = \frac{G_F^2}{6\pi^2} M_{W_L}^2 f_K^2 m_K \kappa \sum_{\gamma, \delta=1}^6 \text{Re}(\Lambda_\gamma^{LR} \Lambda_\delta^{RL}) 2\beta \sqrt{x_\gamma x_\delta} F(x_\gamma, x_\delta, \beta), \quad (82)$$

where

$$\langle \bar{K}^0 | (\bar{s}Ld)(\bar{s}Rd) | K^0 \rangle = \frac{1}{3} \kappa f_K^2 m_K, \quad (83)$$

with

$$\kappa = \frac{3}{4} \frac{m_K^2}{(m_s + m_d)^2} + \frac{1}{8}. \quad (84)$$

We estimate the matrix element using the vacuum-insertion approximation. In the following estimate of the LR contribution, we neglect the effect of the QCD corrections.

The sum over $\gamma, \delta = 1 \sim 6$ can be reorganized in a better way. By using eq.(67), we obtain

$$c_{Lq_i} c_{Rq_i} \sqrt{x_{q_i}} = -s_{Lq_i} s_{Rq_i} \sqrt{X_{Q_i}}, \quad (i = 1, 2, 3) \quad (85)$$

which lead to a useful formula

$$\begin{aligned} \Delta m_K(LR) &= \frac{G_F^2}{6\pi^2} M_{W_L}^2 f_K^2 m_K \kappa 2\beta \times \\ &\sum_{i,j=1}^3 \text{Re}(\lambda_i^{LR} \lambda_j^{RL}) c_{Lq_i} c_{Rq_i} c_{Lq_j} c_{Rq_j} \sqrt{x_{q_i} x_{q_j}} \tilde{F}(x_{q_i}, x_{q_j}, X_{Q_i}, X_{Q_j}, \beta), \end{aligned} \quad (86)$$

where

$$\tilde{F}(x_{q_i}, x_{q_j}, X_{Q_i}, X_{Q_j}, \beta) = F(x_{q_i}, x_{q_j}, \beta) - F(X_{Q_i}, x_{Q_j}, \beta) - F(x_{q_i}, X_{Q_j}, \beta) + F(X_{Q_i}, X_{Q_j}, \beta), \quad (87)$$

which is a gauge invariant quantity [21]. λ_i^{LR} is defined by

$$\lambda_i^{LR} = U_{q_i d}^{L*} U_{q_i s}^R, \quad (i = 1, 2, 3). \quad (88)$$

Before closing this sub-section, we show the SM contribution $M_{12}^K(LL)$, which is used in the following calculations:

$$\begin{aligned} M_{12}^K(LL) &= \frac{G_F^2}{12\pi^2} F_K^2 B_K m_K M_{W_L}^2 [(\lambda_c^{LL})^2 \eta_1 S(x_c) + (\lambda_t^{LL})^2 \eta_2 S(x_t) + 2\lambda_c^{LL} \lambda_t^{LL} \eta_3 S(x_c, x_t)], \\ \lambda_i^{LL} &= U_{q_i d}^{L*} U_{q_i s}^L, \quad (i = 1, 2, 3), \end{aligned} \quad (89)$$

where $S(x)$ and $S(x, y)$ are the Inami-Lim functions, and $\eta_1 = 1.38$, $\eta_2 = 0.57$ and $\eta_3 = 0.47$ are used. The parameter B_K is taken to be 0.75 ± 0.15 in the following calculations.

6.2 Numerical results in LR symmetric limit

In the limit of $m_u = 0$, the up flavors contribution, i.e., the (i=u and/or j=u) contribution to $\Delta m_K(LR)$ vanishes. The loop integrated functions $\tilde{F}(x_i, x_j, X_i, X_j, \beta)$ for charm flavors, top flavors and the mixed flavors intermediate states are given approximately as:

$$\begin{aligned}\tilde{F}(x_c, x_c, X_C, X_C, \beta) &\simeq 5 + 4 \ln x_c - \ln y_c + \ln \beta, \\ \tilde{F}(x_t, x_t, X_T, X_T, \beta) &\simeq \frac{4 - x_t}{1 - x_t} + \frac{x_t^2 - 2x_t + 4}{(1 - x_t)^2} \ln x_t + \ln \beta, \\ \tilde{F}(x_c, x_t, X_C, X_T, \beta) &\simeq \frac{4 - x_t}{1 - x_t} \ln x_t + \ln \beta,\end{aligned}\tag{90}$$

where $y_i = \beta X_i = m_{Q_i}^2 / M_{W_R}^2$. The contribution of each intermediate state also depends on the mixings:

$$\lambda_i^{LR} \lambda_j^{RL} = U_{qi d}^{L*} U_{qj s}^R U_{qi s}^{R*} U_{qj d}^L. \tag{91}$$

In the left-right symmetric limit of the Yukawa couplings, i.e. $y_{L(U,D)} = y_{R(U,D)}$ in eq.(60), the relations $U_{qi d}^L = U_{qi d}^R$ and $U_{qi s}^L = U_{qi s}^R$ hold. As we discussed in the section 5, we can apply the Wolfenstein parameterization on U^L and U^R . Taking into consideration these mixing matrices, we can estimate contributions of charm flavors, top flavors and mixed flavors of charm and top flavors intermediate states. The charm flavor contribution includes (c,c), (c,C), (C,c) and (C,C) as intermediate states. The top flavor contribution includes (t,t), (t,T), (T,t) and (T,T). The mixed flavor contribution comes from (c,t), (C,t), (c,T), and (C,T) intermediate states. The relative contributions of ordinary quarks and singlet quarks are found by estimating $\tilde{F}(x_{q_i}, x_{q_j}, X_{Q_i}, X_{Q_j}, \beta)$. Using the Wolfenstein parameterization, the mass difference $\Delta m_K(LR)$ is given by,

$$\begin{aligned}\frac{\Delta m_K(LR)}{\Delta m_K} &= 2\sqrt{2} C_\epsilon \kappa \beta \{ \lambda^2 x_c \tilde{F}(x_c, x_c, X_C, X_C, \beta) \\ &\quad + A^4 \lambda^{10} \{ (1 - \rho)^2 - \eta^2 \} x_t c_{Rt}^2 \tilde{F}(x_t, x_t, X_T, X_T, \beta) \\ &\quad + 2A^2 \lambda^6 (1 - \rho) \sqrt{x_c x_t} c_{Rt} \tilde{F}(x_c, x_t, X_C, X_T, \beta) \}, \\ C_\epsilon &= \frac{G_F^2 F_K^2 m_K M_{WL}^2}{6\sqrt{2}\pi^2 \Delta m_K} = 3.78 \times 10^4.\end{aligned}\tag{92}$$

$x_c \tilde{F}(x_c, x_c, X_C, X_C, \beta) \simeq -0.015$, $x_t \tilde{F}(x_t, x_t, X_T, X_T, \beta) \simeq -14$ and $\sqrt{x_c x_t} \tilde{F}(x_c, x_t, X_C, X_T, \beta) \simeq 0.018$ for $M_{W_R} = 2(\text{TeV})$. So, it is found that the charm flavor contribution is the most important in $\Delta m_K(LR)$. We also note that the $W_L - W_R$ box graph contribution to Δm_K is negative relative to the $W_L - W_L$ one. Among the charm flavor contributions, a quarter of the $\Delta m_K(LR)$ comes from two isosinglet quark intermediate states, i.e., (C,C). This can be seen that the singlet C quark intermediate states contribution in $\tilde{F}(x_c, x_c, X_C, X_C, \beta)$ is approximately given by $1 - \ln y_c + \ln \beta$. In the numerical calculation, we must give the mass of the isosinglet quark C. It is determined as follows. The mass of charm quark is given by the seesaw formulae, $m_c \cong (\eta_R / m_C) y_{RU2} y_{LU2} \eta_L$. In the left-right symmetric limit, i.e., $y_{RU2} \cong y_{RU2} = y_{U2}$, it becomes, $m_c = 2(\frac{y_{U2}}{g})^2 \frac{M_{WR} M_{WL}}{m_C}$. With the assumption of the strength of Yukawa coupling,

$y_{U2} = O(g)$, we get $m_C = O(100 \times M_{WR})$. In our numerical calculation of Δm_K and ϵ_K , we set $m_C = 100M_{WR}$. The $W_L - W_L$ box graph contribution is well known and is given by

$$\frac{\Delta m_K(LL)}{\Delta m_K} = \sqrt{2}C_\epsilon B_K \lambda^2 x_c \eta_1. \quad (93)$$

The $W_L - W_R$ box graph contribution to Δm_K is negative relative to the $W_L - W_L$ one. Therefore the experimental value of K_L and K_S mass difference can be fitted only if there is sizable constructive contribution to Δm_K due to the long distance effects or if W_R is sufficiently large and Δm_K is saturated by the standard model like contribution. Including possible long distance effects, Δm_K consists of three parts.

$$\Delta m_K = \Delta m_K(LL) + \Delta m_K(LR) + \Delta m_{Long}, \quad (94)$$

where Δm_{Long} is the long distance contribution. First, we show the ratio $\frac{\Delta m_K(LR)}{\Delta m_K(LL)}$ versus M_{WR} in Fig.2, where $m_s = 120\text{MeV}$ or 200MeV , and $B_K = 0.75$ are used. In order for the $W_L - W_R$ contribution to be smaller than the $W_L - W_L$ one, $M_{WR} \geq 1.3\text{TeV}$ should be satisfied. In Fig.3, we show the Δm_{Long} which is needed to explain the experimental value Δm_K in the present model. If we allow the sizable $\Delta m_{Long} = O(\Delta m_K)$, M_{WR} is allowed to be 1TeV . Therefore we conclude the lower bound for M_{WR} obtained from Δm_K is $O(1\text{TeV})$, though there is large theoretical uncertainty on the lower bound on M_{WR} from K_L and K_S mass difference.

6.3 CP violation

Let us discuss the CP violation of the $K^0 - \bar{K}^0$ system. By studying ϵ_K in the present model, we can obtain alternative constraint on two important parameters M_{WR} and M_T in the model. As we discussed in the previous sub-section, the lower bound on M_{WR} is obtained from Δm_K . However it is shown that K_L and K_S mass difference is not sensitive to M_T because the top flavors contribution is tiny in the real part of M_{12} . However, in the imaginary part, the top flavors contribution becomes important as M_T is larger. Neglecting tree level FCNC, there is one CP violating phase for the left-handed mixing matrix U^L and one for the right-handed mixing matrix U^R . In the left-right symmetric limit, $U^L = U^R$ holds and we have only one CP violating phase. The CP violating effect of the $W_L - W_R$ exchange in the $K^0 - \bar{K}^0$ mixing is proportional to the CP violating phase. The imaginary part of M_{12}^K , which comes from $W_L - W_R$ exchanged diagrams is given as follows:

$$\begin{aligned} \text{Im} M_{12}^K(LR) &= \frac{G_F^2}{12\pi^2} M_{W_L}^2 f_K^2 m_K \kappa 2\beta \times \\ &\quad \sum_{i,j=1}^3 \text{Im}(\lambda_i^{LR} \lambda_j^{RL})_{cLq_i cRq_i cLq_j cRq_j} \sqrt{x_{q_i} x_{q_j}} \tilde{F}(x_{q_i}, x_{q_j}, X_{Q_i}, X_{Q_j}, \beta) \end{aligned} \quad (95)$$

where

$$\text{Im}(\lambda_c^{LR} \lambda_c^{RL}) = -2A^2 \lambda^6 \eta, \quad \text{Im}(\lambda_t^{LR} \lambda_t^{RL}) = 2A^4 \lambda^{10} \eta (1 - \rho), \quad \text{Im}(\lambda_c^{LR} \lambda_t^{RL}) = 2A^2 \lambda^6 \eta. \quad (96)$$

ϵ_K in the present model can be written as,

$$\begin{aligned}
\epsilon_K &= \epsilon_{LL} + \epsilon_{LR}, \\
\epsilon_{LR} &= C_\epsilon \kappa \beta \eta \{ -2A^2 \lambda^6 x_c \tilde{F}(x_c, x_c, X_C, X_C, \beta) + 2A^4 \lambda^{10} (1 - \rho) c_{Rt}^2 x_t \tilde{F}(x_t, x_t, X_T, X_T, \beta) \\
&\quad + 2A^2 \lambda^6 \sqrt{x_c x_t} c_{Rt} \tilde{F}(x_c, x_t, X_C, X_T, \beta) \} \exp(i\frac{\pi}{4}), \\
\epsilon_{LL} &= \frac{1}{2} B_K C_\epsilon \eta \{ -2A^2 \lambda^6 \eta_1 S(x_c, x_c) + 2A^4 \lambda^{10} \eta_2 (1 - \rho) S(x_t, x_t) \\
&\quad + 2A^2 \lambda^6 \eta_3 S(x_c, x_t) \} \exp(i\frac{\pi}{4}).
\end{aligned} \tag{97}$$

For numerical calculation, we must know how c_{Rt} and m_T depend on the parameters M_T and M_{W_R} . In the present model, the masses of the top quark and its singlet partner are given by,

$$m_t \cong \sqrt{2} \left(\frac{|y_L y_R|}{g^2} \right) M_{W_L} \frac{1}{\sqrt{\left(\frac{|y_R|}{g} \right)^2 + \left(\frac{M_T}{\sqrt{2} M_{W_R}} \right)^2}}, \tag{98}$$

$$m_T \cong \sqrt{2} M_{W_R} \sqrt{\left(\frac{|y_R|}{g} \right)^2 + \left(\frac{M_T}{\sqrt{2} M_{W_R}} \right)^2}. \tag{99}$$

(c.f. Eq.(9)). In the case of the left-right symmetric limit $y_L = y_R \equiv y$, the Yukawa coupling y is given in terms of the top quark mass:

$$y^2 = g^2 \frac{m_t^2}{4M_{W_L}^2} \left(1 + \sqrt{1 + 4 \frac{M_{W_L}^2 M_T^2}{M_{W_R}^2 m_t^2}} \right). \tag{100}$$

Then the singlet quark mass is given as

$$m_T = m_t \frac{M_{W_R}}{M_{W_L}} \frac{1}{2} \left(1 + \sqrt{1 + 4 \frac{M_{W_L}^2 M_T^2}{M_{W_R}^2 m_t^2}} \right). \tag{101}$$

In the case of $M_{W_R} \gg M_T$, we get $m_T \simeq m_t M_{W_R}/M_{W_L}$. Thus, the physical mass of the singlet T quark is determined if M_{W_R} and M_T are fixed. In Fig.4, we show the magnitude of Yukawa coupling in the region of $M_T \leq M_{W_R}$. The Yukawa coupling increases as M_T is larger. Increasing M_T further may invalidate the perturbative calculation. In Fig.5, c_{Rt} is shown versus M_T/M_{W_R} . As far as $M_T \ll M_{W_R}$, the singlet-doublet mixing c_{Rt} is approximately given by $c_{Rt} \sim M_T/M_{W_R}$. Coming back to ϵ_K , the top flavor contribution is suppressed by the factor. Such suppression mechanism is distinctive in the present left-right model. c_{Rt} increases as M_T is larger. So the top flavor contribution is more important as M_T increases.

There are two distinctive cases on the contribution to ϵ parameters. One corresponds to the case that $\frac{\epsilon_{LR}}{\epsilon_{LL}}$ is positive and the other corresponds to $\frac{\epsilon_{LR}}{\epsilon_{LL}}$ is negative. The ratio is shown as a function of M_T in Fig.6, where $M_{W_R} = 0.5, 1.5$, and 3 TeV are taken. The ratio does not depend on η and we set $\rho = 0$. As seen in this figure, the LR contribution is negative in $M_T \geq 60$ GeV, but positive in $M_T \leq 60$ GeV relative to LL contribution. (See Eq.(97).) If

$\epsilon_{LR} \neq 0$ and we would use the standard model expression to fit ϵ_K , i.e., with $\epsilon_K = \epsilon_{LL}(\rho, \eta)$, there would be disagreement between the allowed region of (ρ, η) determined by B physics data only and that obtained by ϵ_K . Specifically, here we mean $|V_{ub}|$, $|V_{cb}|$ from semileptonic B decays and $|V_{td}|$ from $B\bar{B}$ mixing as B physics data. When we obtain the constraint on $|V_{td}|$ from the $B\bar{B}$ mixing, we can use the SM expression for M_{12} because the deviation from the SM in $W_L W_L$ exchanged diagrams are negligible for the small mixing angle $s_{Lt} = O((\frac{M_{WL}}{M_{WR}})^2)$ and $W_R W_L$ exchanged diagrams do not contribute to $B\bar{B}$ mixing as we show later. After all, for the small mixing angle case, the B physics data is not affected by the presence of the new physics. Then the mismatch between the constraint of ϵ_K and that of the B physics data will be manifested in the following ways.

- (1) The (ρ, η) determined by the B physics data is above the line obtained from the constraint $\epsilon_K = \epsilon_{LL}(\rho, \eta)$. This case corresponds to $\epsilon_{LR}/\epsilon_{LL} < 0$.
- (2) The (ρ, η) determined by the B physics data is below the line obtained from the constraint $\epsilon_K = \epsilon_{LL}(\rho, \eta)$. This case corresponds to $\epsilon_{LR}/\epsilon_{LL} > 0$.

Qualitatively, this mismatch is understood as follows. If the CP violating parameter η determined by the B physics data is larger than the one determined by the standard model constraint $\epsilon_K = \epsilon_{LL}$, we need some negative contribution to ϵ_K relative to ϵ_{LL} . If the η determined by the B physics data is smaller, then the ϵ_{LL} is not enough to explain ϵ_K and we need positive contribution to ϵ_K . The present data of $B_d \bar{B}_d$ mixing and $|V_{ub}|$ as well as the bag parameters B_K and B_B are not sufficiently accurate to discriminate the one case from the others. Of course, this mismatch may disappear by using the full expression for ϵ_K in the present model with the parameters M_T and M_{WR} suitably adjusted. In Fig.7, we show the allowed region for $(M_{WR}, \frac{M_T}{M_{WR}})$ using the full expression for ϵ_K ,

$$\epsilon_K = \epsilon_{LL}(\rho, \eta) + \epsilon_{LR}(\rho, \eta, M_{WR}, M_T). \quad (102)$$

Taking into account of the present allowed region for (ρ, η) obtained from $B_d \bar{B}_d$ mixing, $|V_{cb}|$, $|V_{ub}|$ and ϵ_K , the allowed region for $(M_{WR}, \frac{M_T}{M_{WR}})$ is plotted. Depending on the two cases, the allowed regions of $(M_{WR}, \frac{M_T}{M_{WR}})$ are quite different from each others. The lower curve corresponds to the case (2), i.e., $\frac{\epsilon_{LR}}{\epsilon_{LL}} > 0$. The upper bound on M_{WR} is obtained in this case. The upper curve corresponds to the case (1), i.e., $\frac{\epsilon_{LR}}{\epsilon_{LL}} < 0$. Since η is larger than one which would be obtained by the SM fit, the negative contribution is needed. This is achieved by taking $\frac{M_T}{M_{WR}}$ larger. To maintain this effect while taking M_{WR} larger, $\frac{M_T}{M_{WR}}$ must increase. We use the following experimental inputs to determine the allowed range of (ρ, η) : $|V_{cb}^{\text{CKM}}| = 0.0395 \pm 0.0017$, $m_t = 175.6 \pm 5.5 \text{ GeV}$, $|V_{ub}^{\text{CKM}}/V_{cb}^{\text{CKM}}| = 0.08 \pm 0.016$ and $|V_{td}^{\text{CKM}}| = 0.0084 \pm 0.0018$ [12][23]. We also use $B_K = 0.75$. The above constraints are shown in (ρ, η) plane. (See Fig.9.) In order to find the B_K dependence of our result, we also show the allowed region by taking $B_K = 0.6 \sim 0.9$ with $\rho = 0$ and $\eta = 0.35$ in Fig.8. We can also discuss the $W_L - W_R$ exchange effect on $B_d^0 - \bar{B}_d^0$ mixing. The contribution to $\Delta m_{B_d^0}$ is given as

$$\Delta m_{B_d^0}(LR) = \frac{G_F^2}{6\pi^2} M_{WL}^2 f_{B_d}^2 m_B \kappa 2\beta \times$$

$$\sum_{i,j=1}^3 |\lambda_i^{LR} \lambda_j^{RL}| c_{Lq_i} c_{Rq_i} c_{Lq_j} c_{Rq_j} \sqrt{x_{q_i} x_{q_j}} \tilde{F}(x_{q_i}, x_{q_j}, X_{Q_i}, X_{Q_j}, \beta) , \quad (103)$$

where $\kappa \simeq 3/4$ and

$$\lambda_i^{LR} \lambda_j^{RL} = U_{q_i d}^{L*} U_{q_j b}^R U_{q_i d}^{R*} U_{q_j b}^L . \quad (104)$$

In the SM, the top quark intermediate state dominates the $B_d^0 - \bar{B}_d^0$ mixing. The $W_L - W_R$ exchange contribution is also dominated by the top flavor intermediate state, however, this contribution is suppressed by c_{Rt} , that is of order 10^{-4} compared with the SM contribution. Thus, for $B_d^0 - \bar{B}_d^0$ mixing, the LR effect is negligible.

7 Rare Decays of K Mesons

Experiments in the K meson system have entered a new period with the observation of the rare process $K^+ \rightarrow \pi^+ \nu \bar{\nu}$, and the dedicated search for $K_L \rightarrow \pi^0 \nu \bar{\nu}$. Recently, the signature of the decay $K^+ \rightarrow \pi^+ \nu \bar{\nu}$ has been observed by E787 Collaboration [15] and the reported branching ratio is $4.2_{-3.5}^{+9.7} \times 10^{-10}$, which is consistent with the value predicted by the SM. Additional (and improved) data are expected in the near future. In view of this situation, a detailed study of the rare K meson decays is necessary. The decay $K_L \rightarrow \pi^0 \nu \bar{\nu}$ is one of the most promising processes, since it is a CP violating mode in the SM. This mode is theoretically clean to extract the CKM parameter η [18]. We investigate rare K meson decays in the present model introducing right handed neutrinos. However, in the model, the neutrino masses are zero in the tree level and lepton flavor is well conserved (see analyses within other models [24]). Scalar and tensor operators appear due to the LR box diagrams, in which both the left and right handed gauge bosons, W_L and W_R , are exchanged. The scalar operators have an enhancement factor M_K/m_s in the matrix element $\langle \pi | \bar{s}d | K \rangle$. Thus, the scalar operator may make a large contribution to the rare K meson decays, $K^+ \rightarrow \pi^+ \nu \bar{\nu}$ and $K_{L,S} \rightarrow \pi^0 \nu \bar{\nu}$. An important point is that the CP property of the scalar interaction is different from the V-A interaction $(\bar{s}d)_{V-A}(\bar{\nu}_l \nu_l)_{V-A}$ in the SM. The decay $K_L \rightarrow \pi^0 \nu \bar{\nu}$ through the scalar operator is not a CP violating one, so we have a non-zero branching ratio $B(K_L \rightarrow \pi^0 \nu_l \bar{\nu}_l)$ even in the CP conserved limit ($\eta \rightarrow 0$). Thus, it is important to estimate the size of the effect of the scalar operator on the pion energy spectrum.

7.1 Rare decays by scalar operator

The rare $K \rightarrow \pi \nu \bar{\nu}$ decays are loop-induced FCNC processes in the SM, that, being dominated by short-distance physics, are theoretically very clean modes [18]. The matrix elements involved in these decays are related to the experimentally well known decay $K^+ \rightarrow \pi^0 e^+ \nu$ using isospin symmetry, and corrections to this relation have been studied [25]. We start our analysis of such decays with the following effective Lagrangian, which is produced from the LR box diagram in addition to the SM contributions:

$$\mathcal{L}_{eff} = -\frac{4\kappa G_F}{\sqrt{2}} \sum_{l=e,\mu,\tau} \left[C_{SM}^l (\bar{s}_L \gamma^\mu d_L) (\bar{\nu}_{L,l} \gamma_\mu \nu_{L,l}) \right]$$

$$\begin{aligned}
& + S_{LR}^l (\bar{s}_L d_R) (\bar{\nu}_{L,l} \nu_{R,l}) + S_{RL}^l (\bar{s}_R d_L) (\bar{\nu}_{R,l} \nu_{L,l}) \\
& + T_{LR}^l (\bar{s}_L \sigma^{\mu\nu} d_R) (\bar{\nu}_{L,l} \sigma_{\mu\nu} \nu_{R,l}) + T_{RL}^l (\bar{s}_R \sigma^{\mu\nu} d_L) (\bar{\nu}_{R,l} \sigma_{\mu\nu} \nu_{L,l}) + h.c. \Big], \quad (105)
\end{aligned}$$

where $\kappa = \alpha/(2\pi \sin^2 \Theta_W)$. The first term is the SM contribution [18, 26], and from the second to the fifth are the new contributions arising in this model. The scalar and tensor operators generally appear from box diagrams when one considers a model which contains the right-handed charged gauge boson W_R . As a concrete analysis, in section 7.3, we investigate the pion energy spectrum for LR symmetric scenario, $S_{LR}^l = S_{RL}^l$ and $T_{LR}^l = T_{RL}^l$, which correspond to the limit $\cos \theta_{Ls} = \cos \theta_{Rd} = 1$ with $U^R = U^L$.

There are also penguin diagram contributions to the process we are interested in. However, only the box diagrams produce the scalar operator $(\bar{s}d)_S(\bar{\nu}\nu)_S$ in the effective Lagrangian, thus, we do not consider the contributions from penguin diagrams in this paper.

First we show the decay amplitudes for the neutral K meson states K_L and K_S ¹. The decay amplitudes $A(K_{L,S} \rightarrow \pi^0 \bar{\nu} \nu)$ are:

$$\begin{aligned}
A(K_{L,S} \rightarrow \pi^0 \bar{\nu}_l \nu_l) = & -\frac{G_F \kappa}{\sqrt{2}} \left((p C_{SM}^l \mp q C_{SM}^{l*}) \langle \bar{s} \gamma^\mu d \rangle (\bar{\nu}_l \gamma_\mu (1 - \gamma_5) \nu_l) \right. \\
& + (p(S_{LR}^l + S_{RL}^l) \pm q(S_{LR}^l + S_{RL}^l)^*) \langle \bar{s} d \rangle (\bar{\nu}_l \nu_l) \\
& + (p(S_{LR}^l - S_{RL}^l) \mp q(S_{LR}^l - S_{RL}^l)^*) \langle \bar{s} d \rangle (\bar{\nu}_l \gamma_5 \nu_l) \\
& + 4(p(T_{LR}^l + T_{RL}^l) \mp q(T_{LR}^l + T_{RL}^l)^*) \langle \bar{s} \sigma^{\mu\nu} d \rangle (\bar{\nu}_l \sigma_{\mu\nu} \nu_l) \\
& \left. + 4(p(T_{LR}^l - T_{RL}^l) \pm q(T_{LR}^l - T_{RL}^l)^*) \langle \bar{s} \sigma^{\mu\nu} d \rangle (\bar{\nu}_l \sigma_{\mu\nu} \gamma_5 \nu_l) \right) \quad (106)
\end{aligned}$$

The CP conserved limit corresponds to $p = q$, with all coefficients $C_{SM}^l, S_{LR}^l, S_{RL}^l, T_{LR}^l$ and T_{RL}^l real. In this limit, the decay amplitude $A(K_L \rightarrow \pi^0 \bar{\nu}_L \nu_L)$ through the V-A interaction is zero, while $A(K_S \rightarrow \pi^0 \bar{\nu}_L \nu_L)$ is nonzero, and the decays through the scalar operators $A(K_{L,S} \rightarrow \pi^0 \bar{\nu}_R \nu_L, \pi^0 \bar{\nu}_L \nu_R)$ remain non-zero generally. In the LR symmetric parameterization, K_S decay through the scalar operators is the CP violating mode, while CP is conserved for K_L decay. Thus decays of neutral K meson in the LR symmetric parameterization are summarized as follows:

$$\begin{aligned}
\bullet K_L \text{ decay} \quad & \begin{cases} (\bar{s}d)_{V-A}(\bar{\nu}_l \nu_l)_{V-A} & \Rightarrow C/\mathcal{P} \\ (\bar{s}d)_S(\bar{\nu}_l \nu_l)_S & \Rightarrow CP \text{ Conserving} , \\ (\bar{s}d)_T(\bar{\nu}_l \nu_l)_T & \Rightarrow C/\mathcal{P} \end{cases} \\
\bullet K_S \text{ decay} \quad & \begin{cases} (\bar{s}d)_{V-A}(\bar{\nu}_l \nu_l)_{V-A} & \Rightarrow CP \text{ Conserving} , \\ (\bar{s}d)_S(\bar{\nu}_l \nu_l)_S & \Rightarrow C/\mathcal{P} \\ (\bar{s}d)_T(\bar{\nu}_l \nu_l)_T & \Rightarrow CP \text{ Conserving} . \end{cases}
\end{aligned}$$

Experimentally we do not observe the neutrinos, and the pion energy spectrum is obtained by summing these contributions which have different CP properties with each other. The K_L decay through the V-A operator is suppressed due to CP symmetry, but decays through

¹We use a conventional phase choice where $|K_{L,S}\rangle \equiv p|K^0\rangle \pm q|\bar{K}^0\rangle$, $CP|K^0\rangle \equiv -|\bar{K}^0\rangle$.

the scalar operators are CP conserving ones, furthermore their matrix elements are enhanced, $\langle \pi^0 | \bar{s}d | K^0 \rangle \sim \frac{M_K^2}{m_s} f^\pm$ (where $\langle (\bar{s}d)_{V-A} \rangle \equiv f_+ p_+^\mu + f_- p_-^\mu, p_\pm = P_K \pm p_\pi$), as we can see from the equation of motion in the next subsection. Thus, the contribution of the scalar interaction to the decay amplitude $A(K_L \rightarrow \pi^0 \nu \bar{\nu})$ is sizable and dominates in the CP conserving limit. The decay amplitude for the charged K meson, $A(K^+ \rightarrow \pi^+ \nu \bar{\nu})$, is obtained in the same way:

$$\begin{aligned}
A(K^+ \rightarrow \pi^+ \bar{\nu}_l \nu_l) = & -\frac{G_F}{\sqrt{2}} \kappa (C_{SM} \langle \bar{s} \gamma^\mu d \rangle (\bar{\nu}_l \gamma_\mu (1 - \gamma_5) \nu_l) \\
& + (S_{LR} + S_{RL}) \langle \bar{s} d \rangle (\bar{\nu}_l \nu_l) \\
& + (S_{LR} - S_{RL}) \langle \bar{s} d \rangle (\bar{\nu}_l \gamma_5 \nu_l) \\
& + 2(T_{LR} + T_{RL}) \langle \bar{s} \sigma^{\mu\nu} d \rangle (\bar{\nu}_l \sigma_{\mu\nu} \nu_l) \\
& + 2(T_{LR} - T_{RL}) \langle \bar{s} \sigma^{\mu\nu} d \rangle (\bar{\nu}_l \sigma_{\mu\nu} \gamma_5 \nu_l)), \tag{107}
\end{aligned}$$

where $\langle \mathcal{O} \rangle = \langle \pi^+ | \mathcal{O} | K^+ \rangle$.

7.2 The matrix elements and the coefficient functions in the LR model

In this section, we explain our estimations of the matrix elements and show explicit forms of the coefficient functions in the LR model. The matrix elements in the SM, $\langle (\bar{s}d)_{V-A} \rangle$, can be related to the matrix elements of the experimentally well known leading decay $K^+ \rightarrow \pi^0 e^+ \nu$ using isospin symmetry. So the form factors $f_\pm^{K^+ \rightarrow \pi^+ \nu \bar{\nu}}$ and $f_\pm^{K^0 \rightarrow \pi^0 \nu \bar{\nu}}$ are written in terms of $f_\pm^{K^0 \rightarrow \pi^0 e^+ \nu}$. The matrix element of the scalar operator $\langle (\bar{s}d)_S \rangle$ is also related to these by the equation of motion:

$$\begin{aligned}
\langle \pi | \bar{s}d | K \rangle &= \frac{p_- \cdot \langle \pi | (\bar{s}d)_{V-A} | K \rangle}{m_d - m_s} \\
&= f_+ \frac{M_K^2 - M_\pi^2}{m_d - m_s} + f_- \frac{p_-^2}{m_d - m_s}, \tag{108}
\end{aligned}$$

where f_\pm are the form factors of the corresponding matrix element $\langle \pi | (\bar{s}d)_{V-A} | K \rangle$. We estimate the matrix element of the tensor operator using the NJL model. First we note that the matrix element of the operator is the second order of the typical momentum. Therefore in the sense of the chiral perturbation, it is enough to estimate the form factor f_T at zero momentum transfer, which is defined by $\langle \bar{s} \sigma^{\mu\nu} d \rangle \equiv \frac{f_T}{M_K} \cdot (p_+^\mu p_-^\nu - p_-^\mu p_+^\nu)$. the SU(3) breaking effect may be also neglected. Calculating the Feynman diagram shown in Fig.10, the form factor is given by

$$f_T = \frac{-i N_c}{4\sqrt{2}\pi^2} \frac{m_q M_K}{f_\pi^2}, \tag{109}$$

where m_q is a constituent quark mass and f_π is the pion decay constant. As a rough order estimate, we assume $m_q = 200$ MeV, $f_\pi = 120$ MeV. Then we obtain, $f_T = -0.37i$. Substituting the value in the pion energy spectrum, we can see that it is safely neglected.

Now we show the explicit form of the coefficient functions S_{LR}^l and T_{LR}^l in the model. We calculate box diagrams, in which the left handed W_L boson and the right handed gauge boson W_R are exchanged, as seen in Fig.7. There are corresponding charged Higgs diagrams due to the gauge invariance. The internal upper fermion lines correspond to the ordinary and the singlet quarks, the lower ones correspond to the SM and the singlet leptons.

The coefficients in the effective Lagrangian are:

$$S_{LR}^l = c_{Ls}c_{Rd} \sum_{q=u,c,t} (U_{qs}^{L*}U_{qd}^R)c_{Lq}c_{Rq} \times \beta \sqrt{x_q y_l} \tilde{F}(x_q, y_l, X_Q, Y_L, \beta), \quad (110)$$

$$T_{LR}^l = -c_{Ls}c_{Rd} \sum_{q=u,c,t} (U_{qs}^{L*}U_{qd}^R)c_{Lq}c_{Rq} \times \beta \sqrt{x_q y_l} \tilde{F}'(x_q, y_l, X_Q, Y_L, \beta). \quad (111)$$

where $\theta_{L/Rq}$ is the mixing angle between a singlet left/right handed quark and the corresponding doublet quark as defined in Eq.(5), and $U_{ij}^{L/R}$ are 3×3 CKM matrix elements. In addition to the parameters x_q, X_Q and β of Eq.(77), new dimensionless parameters y_l, Y_L are defined by:

$$y_l = \frac{m_l^2}{M_{W_L}^2}, \quad Y_L = \frac{m_L^2}{M_{W_L}^2}, \quad (112)$$

where m_l are mass eigenvalues of the ordinary leptons e, μ and τ , while m_L are the corresponding additional heavy lepton masses.

The function \tilde{F}' is defined by replacing $F(x, y, \beta)$ with $F'(x, y, \beta)$ in Eq.(87):

$$F'(x, y, \beta) = \frac{1}{4}I_1(x, y, \beta) - \frac{1+\beta}{16}I_2(x, y, \beta). \quad (113)$$

The other coefficients, S_{RL}^l and T_{RL}^l , can be obtained by interchanging the indices L and R . In the limit when $c_{L,s} = c_{R,d} = 1$, $S_{LR}^l = S_{RL}^l$ and $T_{LR}^l = T_{RL}^l$. Thus, we simply write them as S^l or T^l and take the coefficients as LR symmetric. The coefficients S^l ($l = e, \mu$) for electron and muon are negligibly small due to the smallness of y_e and y_μ , and only S^τ contributes to the process significantly. The coefficient function S^τ evaluated with $M_R = 500$ GeV is:

$$S^\tau \cong -6.10 \times 10^{-7} \lambda_u - 8.76 \times 10^{-5} \lambda_c - 1.46 \times 10^{-3} c_{Rt} \lambda_t, \quad (114)$$

where $\lambda_u \sim \lambda \left(1 - \frac{\lambda^3}{2}\right)$, $\lambda_c \sim -\lambda \left(1 - \frac{\lambda^3}{2}\right)$ and $\lambda_t \sim -A^2 \lambda^5 (1 - \rho - i\eta)$ in the Wolfenstein parameterization. The coefficient for the up quark is negligible. For the top quark, the coefficient function is enhanced by its heavy mass, but suppressed by the CKM factor λ_t , as compared to λ_c from the charm quark. Thus, the contribution from the top quark in the model is small in the case of LR symmetric case. It is important that all the coefficients of the LR model are suppressed by the factor β , so the V-A interaction of the SM dominates as M_R becomes large.

7.3 Pion energy spectrum

We present the pion energy spectrum obtained using the coefficients of Eq.(110) and Eq.(111). In the process $K_L \rightarrow \pi^0 \nu \bar{\nu}$, the contributions from scalar interactions are controlled by β and

the enhancement factor M_K/m_s in the matrix element $\langle(\bar{s}d)\rangle$. For SM, the decay amplitude of $K_L \rightarrow \pi^0 \nu \bar{\nu}$ is proportional to η , thus the contributions of scalar interactions relative to that of SM for the pion energy spectrum is $O\left(\frac{M_K}{m_s} \frac{\beta}{\eta}\right)^2$. In the process $K^+ \rightarrow \pi^+ \nu \bar{\nu}$, contributions from the scalar and tensor interactions are tiny compared to the SM one. The pion energy spectrum for the decay $K^+ \rightarrow \pi^+ \nu \bar{\nu}$ is:

$$\frac{dB(K^+ \rightarrow \pi^+ \nu_l \bar{\nu}_l)}{dx_\pi} = \delta_N \cdot \kappa_+ \sqrt{x_\pi^2 - 4\delta^2} \times \left[(x_\pi^2 - 4\delta^2) (|C_{SM}^l|^2 + 16\omega_+^2 \hat{t} |T^l|^2) + 3\hat{t} \left(\frac{M_K}{m_d - m_s} \right)^2 (1 - \delta^2 + \xi \hat{t})^2 |S^l|^2 \right], \quad (115)$$

$$\kappa_+ = \frac{3\alpha^2 B(K^+ \rightarrow \pi^0 e^+ \nu)}{2\pi^2 \sin^4 \theta_W} \lambda^8 = 4.57 \times 10^{-11}, \quad (116)$$

$$\delta_N = \frac{|f^+(K^+ \rightarrow \pi^0 e^+ \nu)|^2}{\int dx_\pi |f^+(K^+ \rightarrow \pi^0 e^+ \nu)|^2 (x_\pi^2 - 4\delta^2)^{3/2}}, \quad (117)$$

where x_π is a normalized pion energy defined by $x_\pi = 2E_\pi/M_K$, and $\delta = m_\pi/M_K$, $\xi = f_-^{K^+\pi^0}/f_+^{K^+\pi^0}$, $\omega_+ = |f_T^{K^+\pi^0}/f_+^{K^+\pi^0}|$ and $\hat{t} = (1 + \delta^2 - x_\pi)$.

The process $K_L \rightarrow \pi^0 \nu \bar{\nu}$ is a more sensitive probe of the scalar interactions, as discussed in the previous section. The energy spectrum is given by:

$$\frac{dB(K_{L/S} \rightarrow \pi^0 \nu_l \bar{\nu}_l)}{dx_\pi} = \delta_N \cdot \kappa_L \sqrt{x_\pi^2 - 4\delta^2} \times \left[(x_\pi^2 - 4\delta^2) (|pC_{SM}^l \mp qC_{SM}^{l*}|^2 + \omega_0^2 \hat{t} |pT^l \mp qT^{l*}|^2) + 3\hat{t} \left(\frac{M_K}{m_d - m_s} \right)^2 (1 - \delta^2 + \xi \hat{t})^2 |pS^l \pm qS^{l*}|^2 \right], \quad (118)$$

where $\omega_0 \equiv |f_T^{K^0\pi^0}/f_+^{K^+\pi^0}|$ and $\kappa_L = \kappa_+ \cdot \frac{\tau(K_L)}{\tau(K^+)}$. The first term is contributions from V-A and tensor operators, $\bar{s}_{L,R} \sigma^{\mu\nu} d_{L,R}$, the second is the contribution from the scalar operator which has an enhancement factor $M_K^2/(m_d - m_s)^2$ in the matrix element. The contribution from the tensor operator is suppressed by the kinematical factor $(x_\pi^2 - 4\delta^2)$ in the low pion energy region, $x_\pi \sim 2\delta$, whereas at large pion energies, $x_\pi \sim 1 + \delta^2$, it is suppressed by the factor \hat{t} . Furthermore, decay through the tensors is CP violating and has no enhancement factor. Hence, the contribution from the tensor operator is negligible compared to the scalar operator and the SM contributions. The form factors are related to those of the experimentally well known decay mode $K^+ \rightarrow \pi^0 e^+ \nu$. In Fig.12 we show the pion energy spectrum, $\frac{dB(x_\pi)}{dx_\pi}$, multiplied by a factor 10^{10} . To see the dependence of the branching ratio on η , we plotted three curves, which correspond to the cases $\eta = 0.25, 0.3, 0.35$. The solid lines are the pion energy spectra in the LR model, the dotted lines are the corresponding SM prediction, where we have taken $M_{W_R} = 500(\text{GeV})$ and $\rho = 0.25$. The LR contribution is large in the low energy region $x_\pi \sim 2\delta$, while in the high energy region the SM contribution dominates. In Fig.13, we study the dependence of the pion energy spectrum on M_{W_R} . Notice that as the coefficient functions of the effective Lagrangian are proportional to β , dB/dx_π is proportional to $(M_{W_L}/M_{W_R})^4$. The

effect is negligible for $M_{WR} > 1(\text{TeV})$ and the energy spectrum reduces to the prediction of the SM.

The effect of the new physics can be seen in the pion energy spectrum of the $K_L \rightarrow \pi^0 \nu_l \bar{\nu}_l$ decay for $M_{WR} \leq 1 \text{ TeV}$. On the other hand, the analyses of $K^0 - \bar{K}^0$ mixing have given a constraint of $M_{WR} \geq 1.6 \text{ TeV}$, which may discourage the search for new physics in this decay mode. However, it is important to comment on the constraint $M_{WR} \geq 1.6 \text{ TeV}$. This bound has been obtained from the box diagram of the $W_L - W_R$ intermediate state. We assumed, as is usual, that the short distance effect dominates $K^0 - \bar{K}^0$ mixing. However, if long distance physics dominates the mixing, the constraint of $M_{WR} \geq 1.6 \text{ TeV}$ is no longer valid.

8 Conclusion

We present the formalism and systematic analyses of the seesaw model for quark masses. A framework allowing the top quark mass to be of the order of the electroweak symmetry breaking scale is explained. The derivation of the quark mass formulae is presented in detail with flavour mixing included. There, it is shown that expanding simply by the inverse power of the singlet quark mass matrix fails and we propose an alternative expansion to overcome the problem. Furthermore, we find that a quark basis in which the singlet and doublet mixing Yukawa coupling is a triangular matrix is appropriate for finding the mass base. Starting in such a basis, by neglecting the flavor off-diagonal Yukawa couplings, we can reproduce the quark mass formulae which are obtained as the solutions of the eigenvalue equation. Also, we give the theoretical formulae for the tree level FCNC. The tree level FCNC in the model are naturally suppressed as *(quark masses)² divided by an (SU(2) breaking scale)²*. The effect on rare K and B decays is far below both the present experimental bound and the prediction of the standard model. As for FCNC beyond the tree level, the one loop effect involving the right-handed gauge boson exchange is discussed for $K^0 - \bar{K}^0$ mixing and for $K \rightarrow \pi \nu \bar{\nu}$. Δm_K and ϵ_K give constraints on the parameters of the model M_T and M_{WR} . We reanalyse the Beall, Bander and Soni bound for M_{WR} in the present model and show the lower bound of M_{WR} is about $O(1\text{TeV})$. The constraint of ϵ_K is interesting and we show the allowed region in $(M_{WR}, \frac{M_T}{M_{WR}})$. If the allowed region of (ρ, η) is tightened by the data of the B factory and/or by the improvement of the lattice computation of the hadronic matrix element, the allowed region will be much more specified than the present one. Alternatively the effect of the new physics can be seen the $K_L \rightarrow \pi^0 \nu_l \bar{\nu}_l$ decay in the case of $M_{WR} \leq 1(\text{TeV})$. There is a scalar operator in the effective Lagrangian, which come from LR box diagrams. For the decay $K_L \rightarrow \pi^0 \nu \bar{\nu}$, there is a significant contribution from the scalar operator, especially in the low energy region of the pion energy spectrum, which, for the values $M_{WR} = 500\text{GeV}$ and $\rho, \eta = 0.25$, amounts to an enhancement of about 30% to the total branching ratio. Thus, measuring the decay $K_L \rightarrow \pi^0 \nu \bar{\nu}$ precisely may be important to probe the effect from new physics. Other aspects of the present model, such as the constraints from the precision measurements and the other B decays, the Higgs sector, and the neutrino mass and mixings will be discussed elsewhere. The further improvement of the QCD corrections to our computation is also needed for serious comparison with the experiments.

Acknowledgments

We would like to thank G. C. Branco for discussions. One of us (M.T) is also thankful to the High Energy Group in CFIF/IST for their hospitality. This work is supported by the Grant-in-Aid for Joint International Scientific Research (#08044089, Origin of CP and T violation and flavor physics) and the work of T.M. is supported in part by Grant-in-Aid for Scientific Research on Priority Areas (Physics of CP violation).

References

- [1] T. Yanagida, in Proceedings of the Workshop on "The Unified Theory and the Baryon Number of the Universe", Edited by Osamu Sawada and Akio Sugamoto, KEK 13-14 Feb 1979 (KEK-79-18).
- [2] M. Gell-Mann, P. Ramond and R. Slansky in Sanibel Talk, CALT-68-709, Feb. 1979, and in "Supergravity" (North Holland, Amsterdam 1979).
- [3] Z. G. Berezhiani, *Phys. Lett.* **129B** (1983) 99; *Phys. Lett.* **150B** (1985) 177.
- [4] D. Chang, R. N. Mohapatra, *Phys. Rev. Lett.* **58** (1987) 1600.
- [5] J. Rajpoot, *Phys. Lett.* **B191** (1987) 122.
- [6] A. Davidson and K. C. Wali, *Phys. Rev. Lett.* **59** (1987) 393.
- [7] K. S. Babu and R. N. Mohapatra, *Phys. Rev. Lett.* **62** (1989) 1079.
- [8] Y. Koide and H. Fusaoka, *Z. Phys.* **C71** (1996) 459; See also, Y. Koide, in this proceedings, hep-ph/9803458; Y. Koide, *Phys. Rev.* **D56** (1997) 2656-2664.
- [9] T. Morozumi, T. Satou, M. N. Rebelo and M. Tanimoto, *Phys. Lett.* **B410** (1997) 233.
- [10] N. Cabbibo, *Phys. Rev. Lett.* **10** (1963) 531-533.
- [11] M. Kobayashi and T. Maskawa, *Prog. Theor. Phys.* **49** (1973) 652.
- [12] Particle Data Group 1997 edition, <http://pdg.lbl.gov/> .
- [13] S. Glenn et al., *Phys. Rev. Lett.* **80** (1998) 2289-2293.
- [14] A. Ali, G. Hiller, L. Handoko, and T. Morozumi, *Phys. Rev. D* **55** (1997) 4105-4128.
- [15] E787 Collaboration (S. Adler et al.), *Phys. Rev. Lett.* **79** (1997) 2204-2207.
- [16] N. Cabbibo, *Phys. Rev. Lett.* **10** (1963) 531-533.
- [17] M. Kobayashi and T. Maskawa, *Prog. Theor. Phys.* **49** (1973) 652.

- [18] G. Buchalla, A. J. Buras and M. E. Lautenbacher, *Rev. Mod. Phys.* **68** (1996) 1125-1144;
G. Buchalla and A. J. Buras, *Phys. Rev.* **D54** (1996) 6782-6789.
- [19] G. Beall, M. Bander and A. Soni, *Phys. Rev. Lett* **29** (1982) 848.
- [20] G. Ecker and W. Grimus, *Nucl. Phys.* **258B** (1985) 328.
- [21] J. Basecq and L-F. Li and P. B. Pal, *Phys. Rev.* **32D** (1985) 175.
- [22] L. Wolfenstein *Phys. Rev. Lett* **51** (1983) 1945.
- [23] A. J. Buras and R. Fleischer, hep-ph/9704376; to appear in Heavy Flavours II, World Scientific (1997), eds. A.J. Buras and M. Linde.
- [24] See, for example,
A. J. Buras, A. Romanino and L. Silvestrini, *Preprint* hep-ph/9712398; G. Cho, *Preprint* hep-ph/9801406; Y. Grossman and Y. Nir, *Phys. Lett.* **B398** (1997)163-168.
- [25] W. Marciano and Z. Parsa, *Phys. Rev.* **D53** (1996) R1.
- [26] T. Inami and C. S. Lim, *Prog. Theor. Phys.* **65** (1981) 297-314, *ibid.* **65** (1981) 1772.

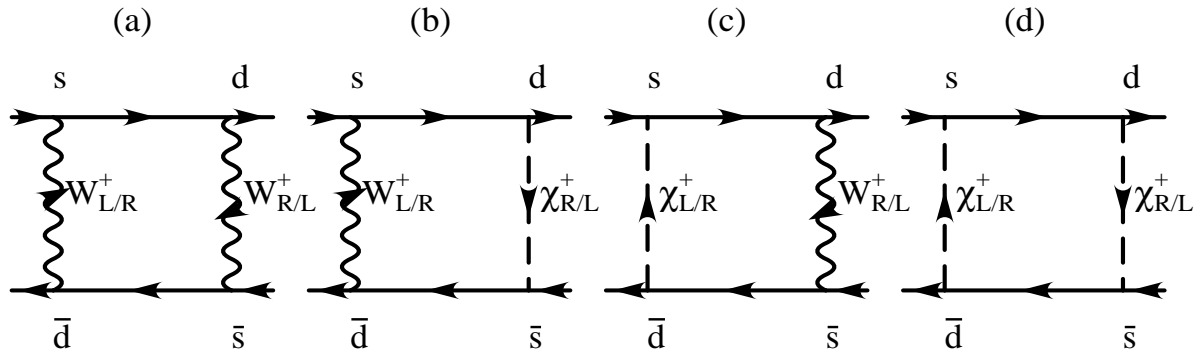


Figure 1: Box diagrams for $K^0 - \bar{K}^0$ mixing involving singlet and doublet quark intermediate states.

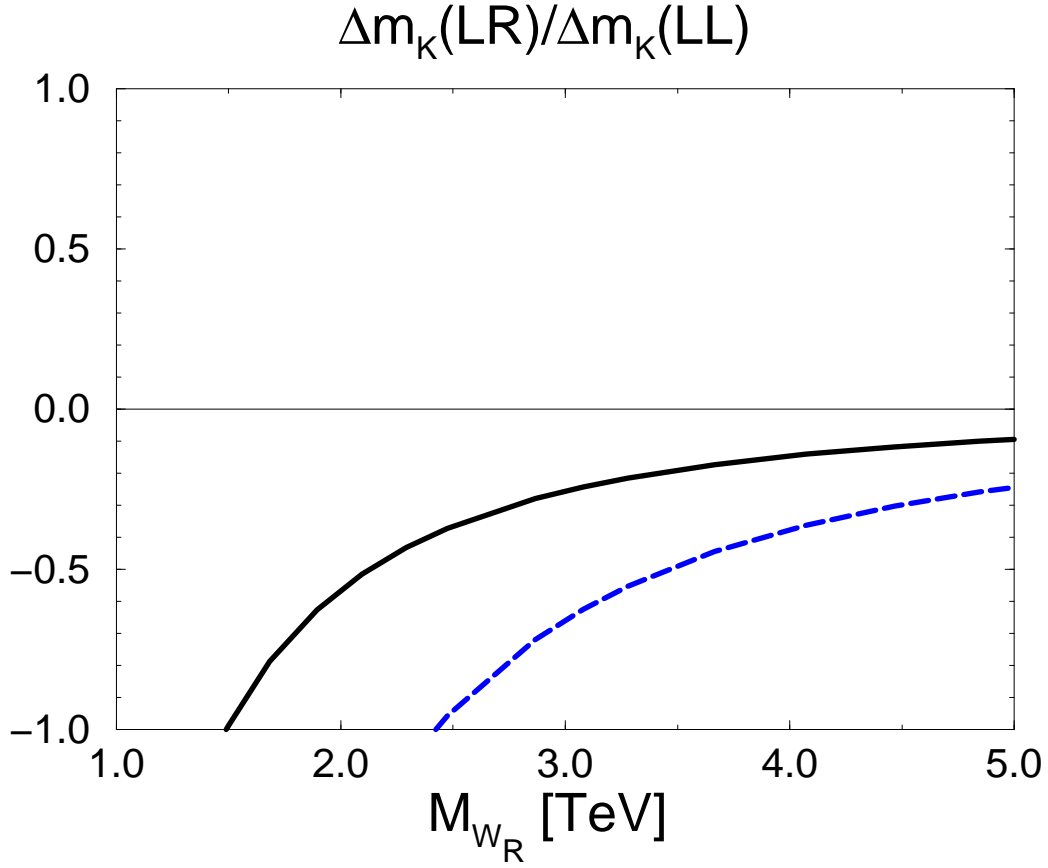


Figure 2: $\frac{\Delta m_K(LR)}{\Delta m_K(LL)}$ as function of M_{WR} . The solid line corresponds to $m_s = 200$ (MeV) and the dashed line corresponds to $m_s = 120$ (MeV). We use $B_K = 0.75$.

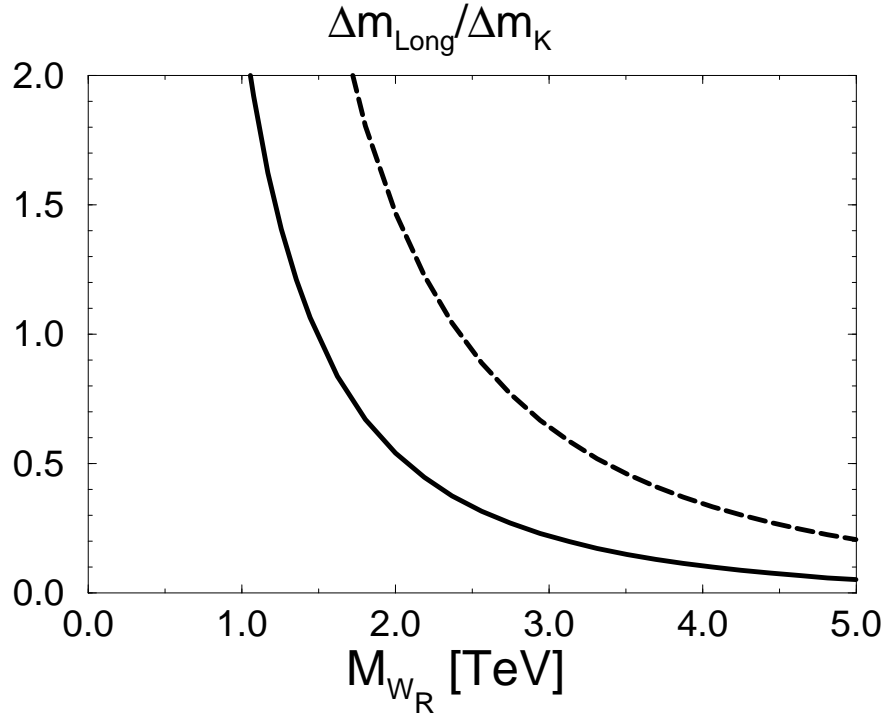


Figure 3: The long distance contribution Δm_{Long} which reproduces the K_L and K_S mass difference in the present model. The solid line corresponds to $m_s = 200(\text{MeV})$ and the dashed line corresponds to $m_s = 120(\text{MeV})$. The unit is the experimental value of Δm_K . We use $B_K = 0.75$.

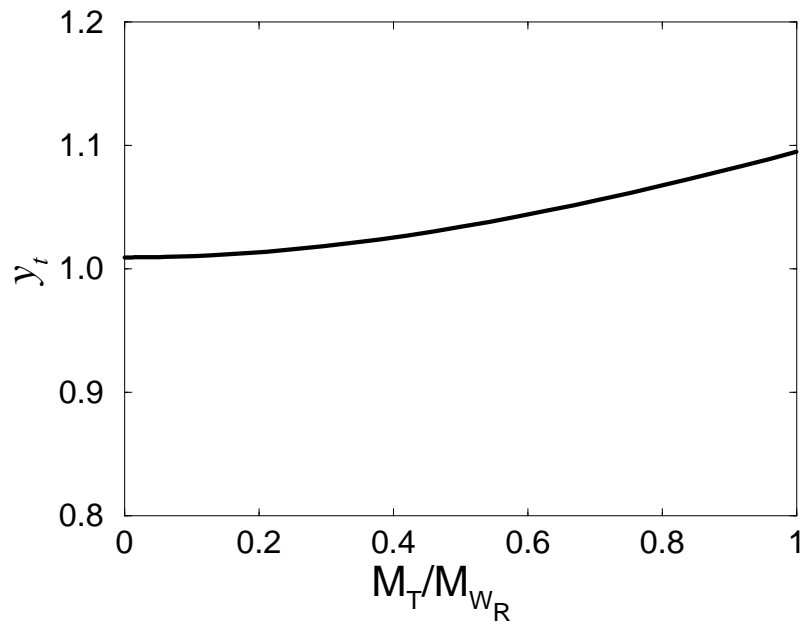


Figure 4: The Yukawa coupling y_t as function of $\frac{M_T}{M_{W_R}}$.

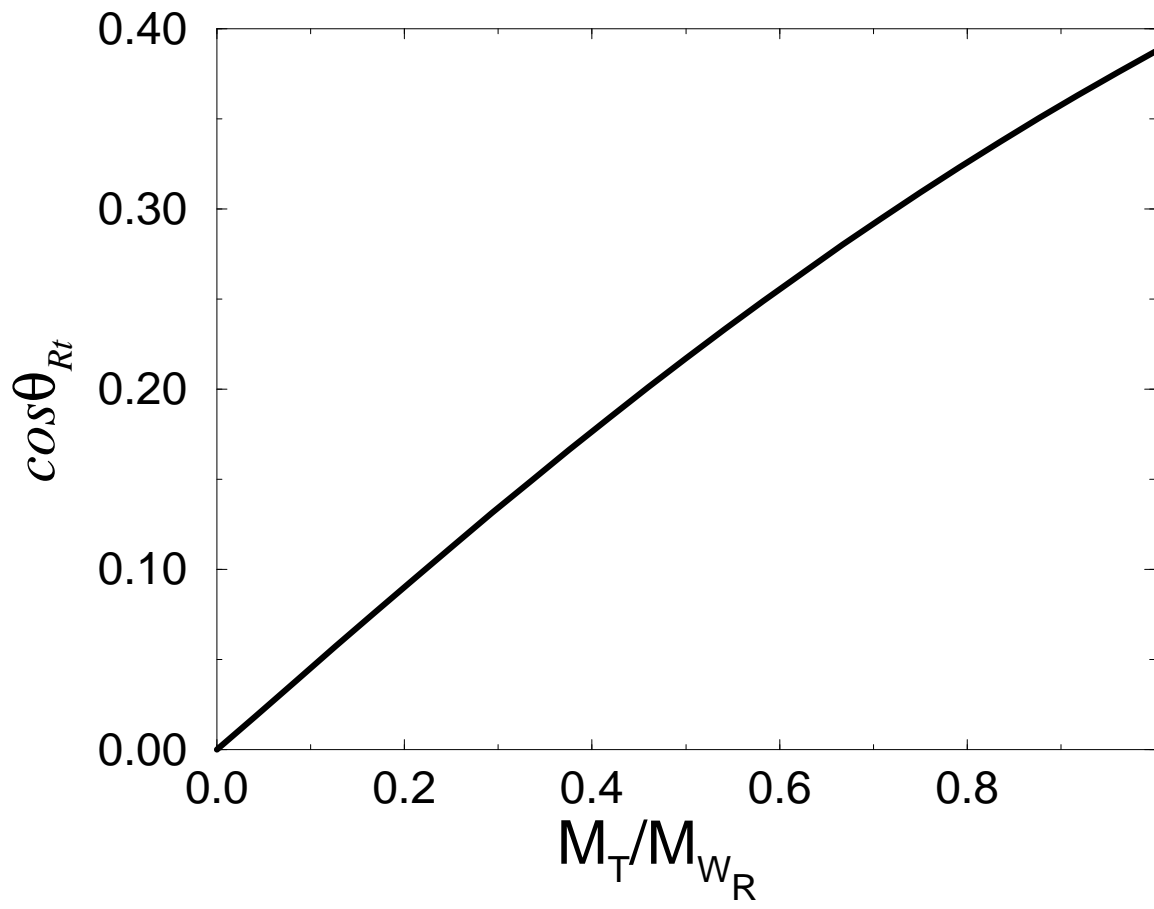


Figure 5: The singlet and doublet mixing angle $\cos \theta_{Rt}$ as function of $\frac{M_T}{M_{WR}}$.

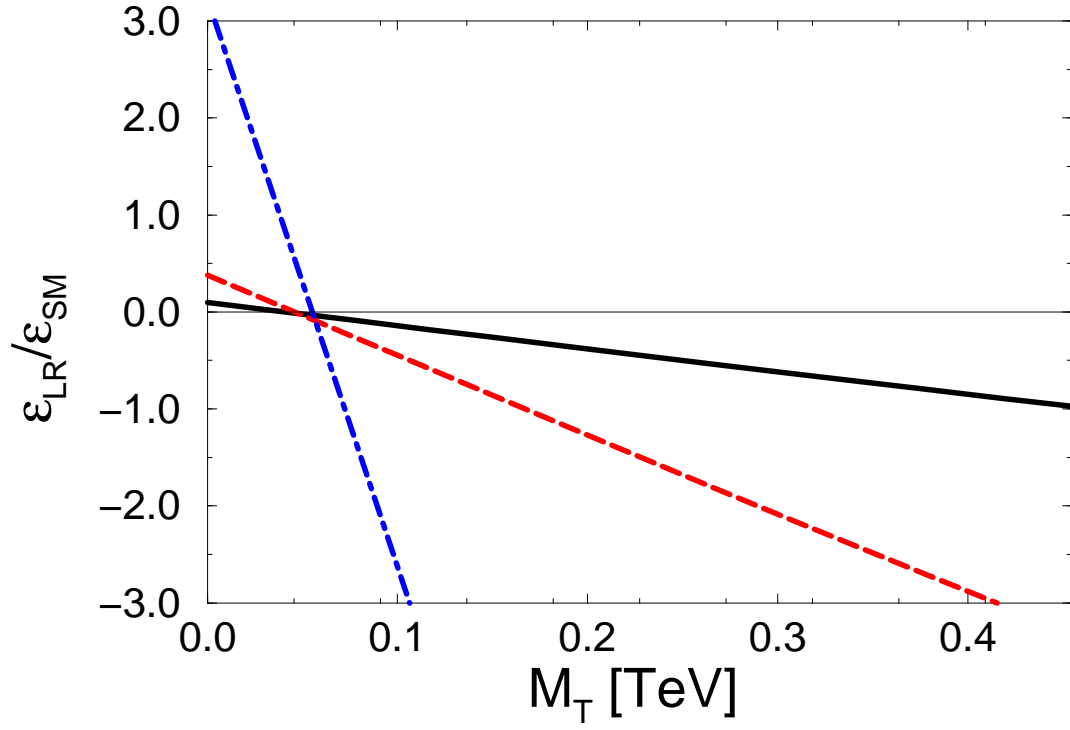


Figure 6: $\frac{\epsilon_{LR}}{\epsilon_{SM}}$ as function of M_T . The solid line corresponds to $M_{WR} = 3(\text{TeV})$, the dashed line corresponds to $M_{WR} = 1.5(\text{TeV})$ and the dotted-dashed line corresponds to $M_{WR} = 0.5(\text{TeV})$. ρ is set to be zero. $m_s = 160(\text{MeV})$ is used.

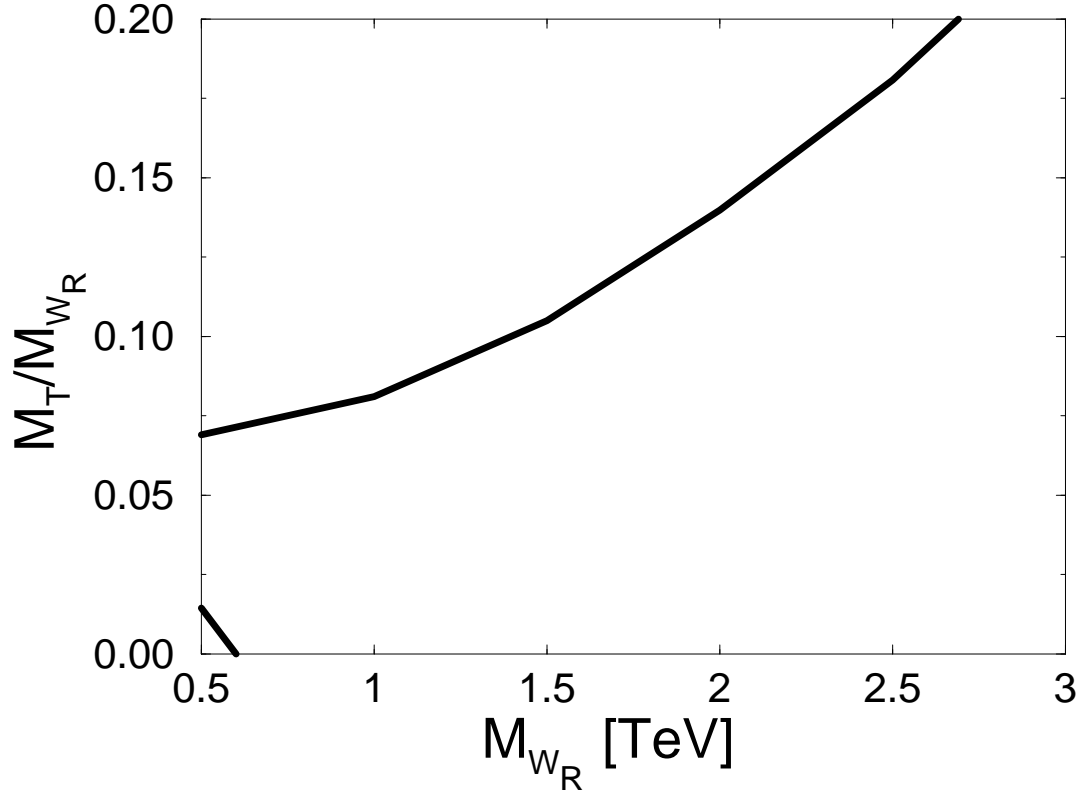


Figure 7: The allowed region for $(M_{WR}, \frac{M_T}{M_{WR}})$. The region between the upper curve and the lower curve is allowed. We take account of the present constraint for (ρ, η) obtained from $B_d \overline{B_d}$ mixing and $|V_{ub}|$. $B_K = 0.75$ and $m_s = 160(\text{MeV})$ are used. The upper curve corresponds to $(\rho, \eta) = (-0.087, 0.43)$ and the lower curve corresponds to $(\rho, \eta) = (0.25, 0.14)$.

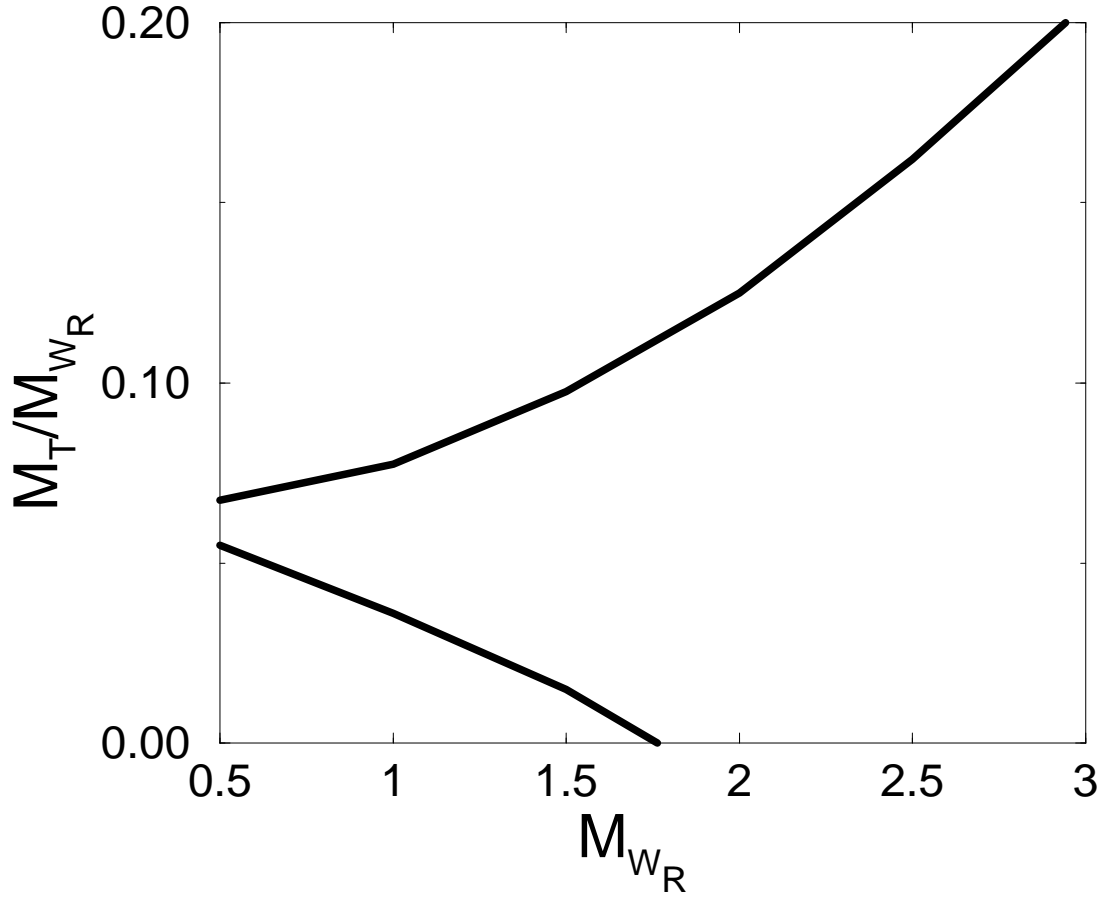


Figure 8: The allowed region for $(M_{WR}, \frac{M_T}{M_{WR}})$ with $(\rho, \eta) = (0, 0.35)$. The lower curve corresponds to $B_K = 0.6$ and the upper curve corresponds to $B_K = 0.9$. The region between two curves is allowed. $m_s = 160(\text{MeV})$ is used.

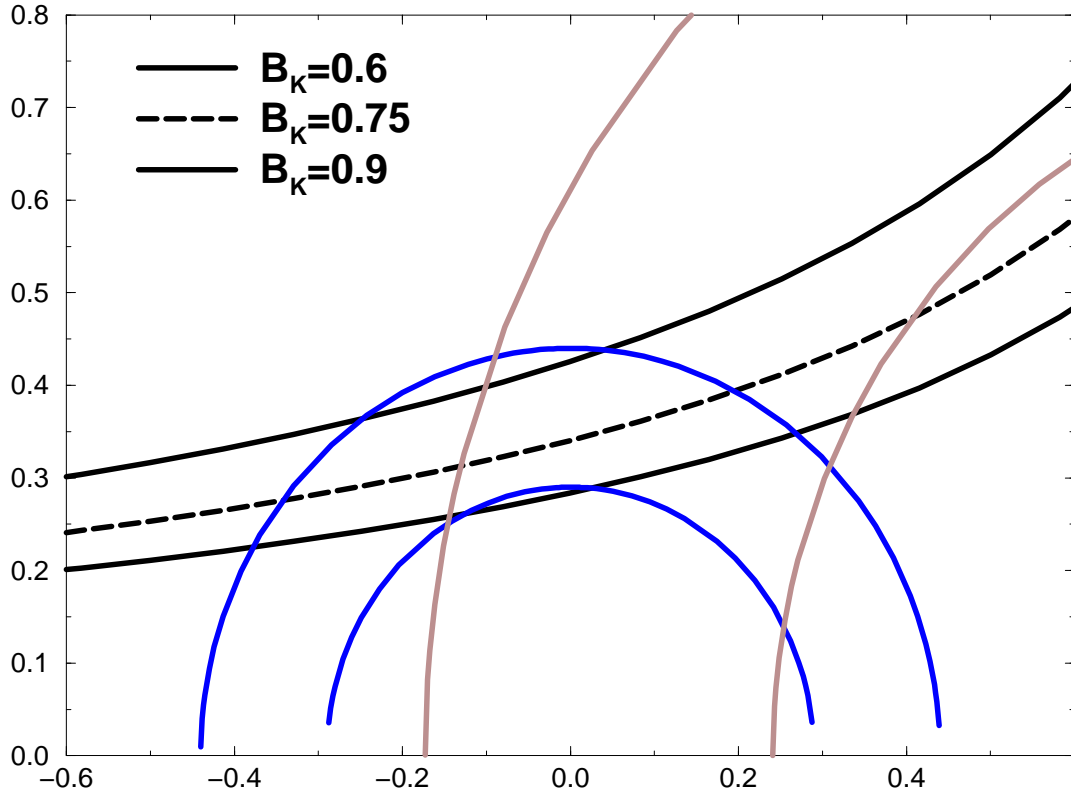


Figure 9: The allowed region in (ρ, η) plane obtained from $|V_{ub}|$, $|V_{cb}|$ and $B_d \bar{B}_d$ mixing. To extract $|V_{td}|$ from $B_d \bar{B}_d$ mixing, we use the SM expression for x_d . This is a good approximation for the small angle case, i.e., $s_{Lt} = O\left(\left(\frac{M_{WL}}{M_{WR}}\right)^2\right)$. (See also the text below Eq.(72).)

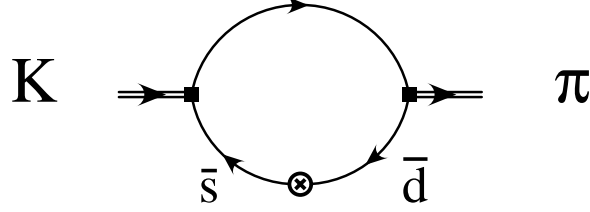


Figure 10: The Feynman diagram for the matrix element of the *tensor* operator in NJL model. \otimes denotes an insertion of the tensor operator $\bar{s}\sigma_{\mu\nu}d$.

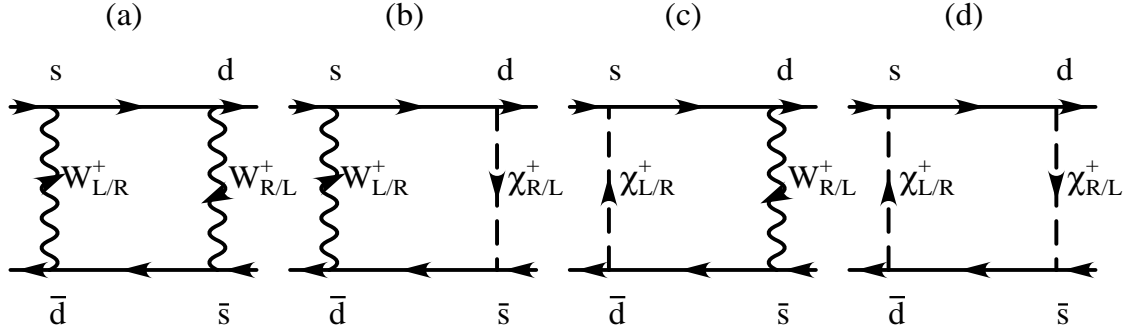


Figure 11: Box diagrams which contribute to the effective Lagrangian for the process $K \rightarrow \pi \nu \bar{\nu}$. (a) is a contribution from W_L and W_R . (b) and (c) are gauge boson and unphysical Higgs contributions. (d) is a contribution from the unphysical Higgs χ_L and χ_R .

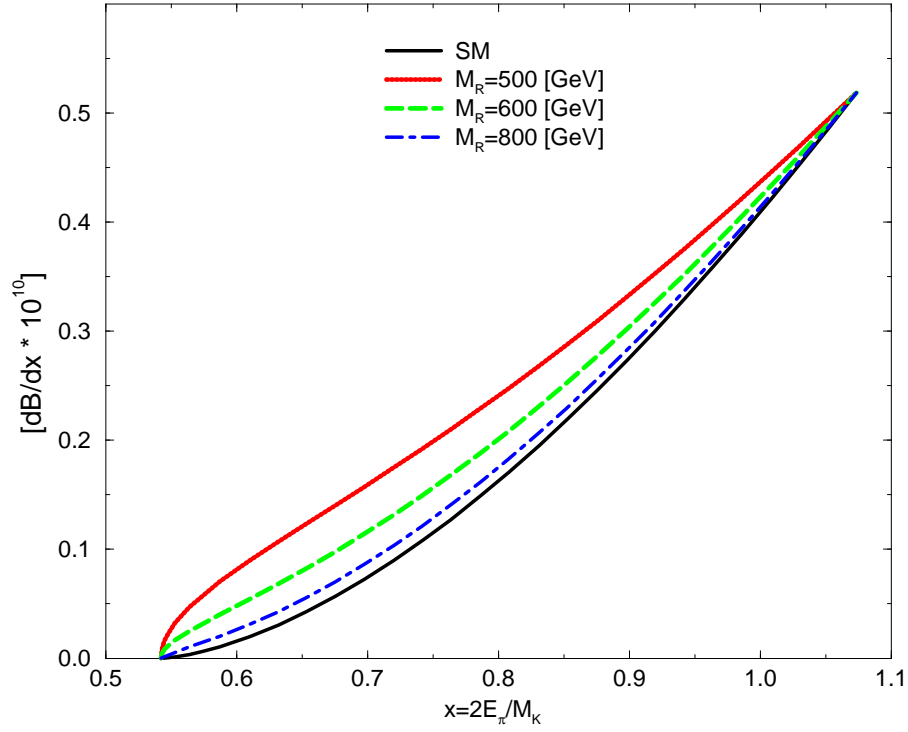


Figure 12: The pion energy spectrum $dB[K_L \rightarrow \pi^0 \nu \bar{\nu}]/dx$ for various values for the CP violating parameter η . We use $m_s = 100(\text{MeV})$, $M_{WR} = 500(\text{GeV})$ and $\rho = 0.25$. SM denotes the predictions of the standard model and LR denotes the predictions of the left-right model.

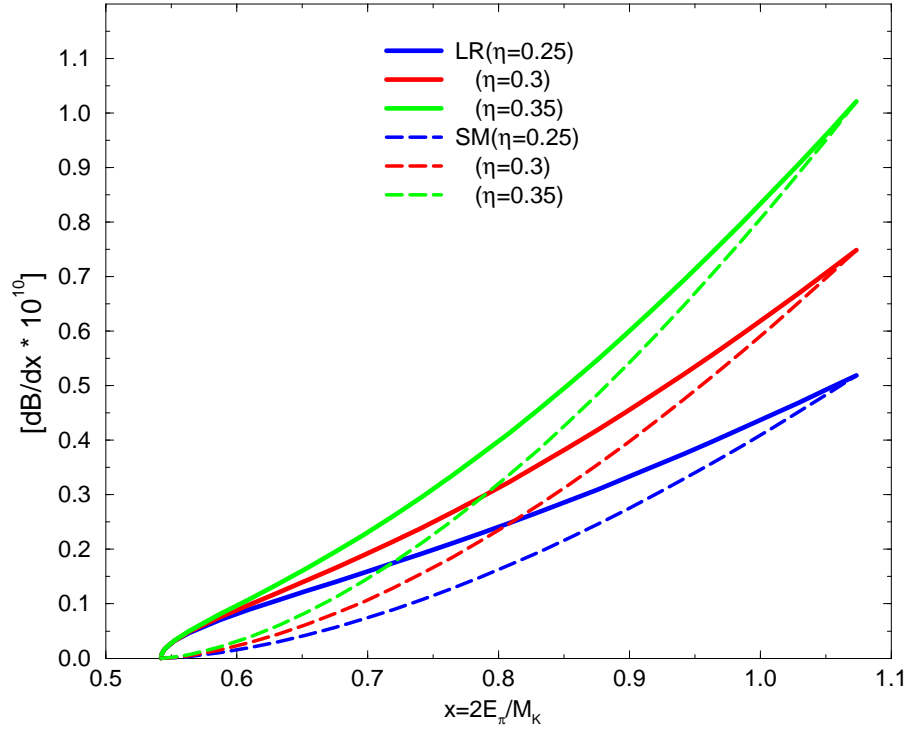


Figure 13: The pion energy spectrum $dB[K_L \rightarrow \pi^0 \nu \bar{\nu}]/dx$ for various values of M_{W_R} . $m_s = 100(\text{MeV})$ is used. SM denotes the prediction of the standard model and LR denotes the predictions of the left-right model.